Journal of Medicinal Chemistry

Article

The first non-discriminating TSPO ligands produced from a carbazole scaffold.

Hei Wun Alison Cheng, Renee Sokias, Eryn Werry, Lars Ittner, Tristan Reekie, Jonathan J. Du, Quanqing Gao, David E Hibbs, and Michael Kassiou

J. Med. Chem., **Just Accepted Manuscript** • DOI: 10.1021/acs.jmedchem.9b00980 • Publication Date (Web): 16 Aug 2019

The first non-discriminating TSPO ligands produced from a carbazole scaffold

Hei Wun Alison Cheng,[◊§] Renee Sokias,[#§] Eryn L. Werry,[#] Lars M. Ittner,[ϕ] Tristan A. Reekie,[#] Jonathan Du,[▽] Quanqing Gao,[▽] David E. Hibbs[▽] and Michael Kassiou.[#]*

[◊]Faculty of Medicine and Health, [#]School of Chemistry and [▽]Sydney School of Pharmacy, Faculty of Medicine and Health, The University of Sydney, NSW, Australia, 2006 [ϕ]Department of Biomedical Sciences, Faculty of Medicine and Health Sciences, 2 Technology Place, Macquarie University, NSW, Australia, 2109.

* Telephone: +61 2 9351 2745. Fax: +61 2 9351 3329. Email: michael.kassiou@sydney.edu.au.

ABSTRACT. Development of neuroinflammation agents targeting the translocator protein (TSPO) has been hindered by a common single nucleotide polymorphism (A147T) at which TSPO ligands commonly lose affinity. To this end, carbazole acetamide scaffolds were synthesized and structure activity relationships elaborated to explore the requirements for high affinity binding to both TSPO wild type (WT) and the polymorphic TSPO A147T. This study reports high binding affinity and non-discriminating TSPO ligands.

KEYWORDS. TSPO, microglia, polymorphism, docking, non-discriminating, structure-activity relationships.

INTRODUCTION

The translocator protein (TSPO), originally named the peripheral benzodiazepine receptor (PBR), is an 18 kDa, five-transmembrane domain protein that is primarily localized on the outer mitochondrial membrane.[1] TSPO is expressed predominantly in steroid-synthesizing tissues, but can also be found in the central nervous system (CNS).[2-3] Specifically, in the non-inflamed CNS, there is low TSPO expression in microglia, the primary immune cells of the CNS.[3] However, upregulation of TSPO expression is evident for activated microglia in areas displaying neuroinflammation, for example in areas damaged by neurodegenerative diseases.[1, 3]

Molecular imaging using positron emission tomography (PET) has been used to assess TSPO expression in preclinical and clinical studies of neurodegenerative diseases.[4] As such, TSPO has become a highly investigated target for the development of therapeutic and diagnostic imaging agents for use in disorders involving neurodegeneration. Development of these drugs, however, has been hindered by the emerging complexity of ligand interactions at the TSPO.

Furthermore, the presence of a single nucleotide polymorphism (SNP; rs6971) in TSPO that results in replacement of an alanine (Ala) with a threonine (Thr) at amino acid residue 147 (A147T) has been reported.[5-6] Human subjects can be clustered into 3 distinct groups based on the ability of second generation TSPO ligands to bind their brain tissue: high-, mixed-, and low-affinity binders. The presence of the predominant TSPO form, Ala/Ala, is associated with high affinity binding, whereas Ala/Thr is associated with mixed affinity binding and Thr/Thr with low-affinity binding.[5-6] The A147T amino-acid substitution results in a conformational change decreasing the affinity of all disclosed TSPO ligands, except PK 11195 (**1**) and the closely related 4-azaisostere **2**.[5-10]

Although the most widely used TSPO PET tracer has been ^{11}C-PK 11195, several major limitations have restricted the clinical use of ^{11}C-PK 11195 in the imaging of neuroinflammation. These limitations include the relatively low brain permeability of ^{11}C-PK 11195 and high nonspecific and plasma protein binding, which result in a low signal-to-noise ratio and low specificity in PET images.[11]

Ultimately, the presence of differing TSPO ligand affinities in the general population complicates the quantitative assessment of PET data, limiting the wide-scale clinical usefulness of this approach.[11] As such, the development of a TSPO ligand that possesses drug-like properties and does not discriminate between the TSPO isoforms would overcome this hurdle. Tricyclics are common core structures of TSPO ligands that display high TSPO affinity and overcome low metabolic stability.[12-13] For example, TSPO ligands, GE-180 (**3**) and SSR-180,575 (**4**), show good brain permeability and TSPO affinity but do discriminate between TSPO isoforms.[12-13] As a result, further investigation into other chemotypes was warranted in our pursuit of non-discriminating TSPO ligands. The carbazole scaffold, whether obtained from natural sources or by synthetic routes, has gained much interest due to its wide range of biological activity upon modifications, including anti-bacterial, anti-malarial, anti-inflammatory, anti-cancer, and anti-Alzheimer properties.[14-16] Given the multifaceted biological properties, the carbazole scaffold was utilized in the design and synthesis of potential TSPO ligands to explore the requirements for high affinity binding to both TSPO wild type (WT) and TSPO A147T.

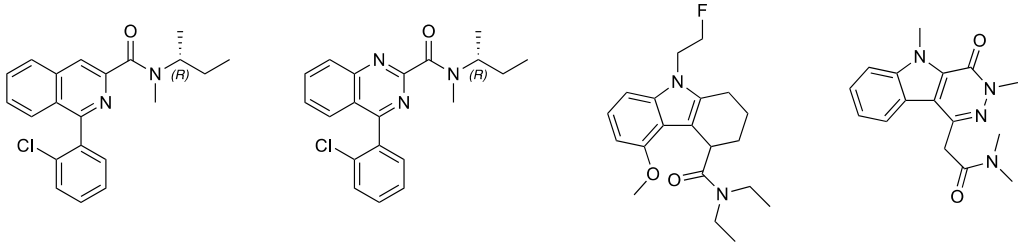

Figure 1. Previously-reported synthetic TSPO ligands PK 11195 (**1**)[17] and 4-azaisostere (**2**),[10] GE-180 (**3**)[12] and SSR-180575 (**4**).[13]

The role of the *N,N*-disubstituted carboxamide was explored as structural studies suggest it may be important for the non-discriminating behavior of PK 11195. In a 3D structure of mammalian TSPO resolved using NMR, the substituents on the carboxamide nitrogen of PK 11195 interact with residues in the 1st trans-membrane segment of TSPO (e.g. A23 and V26), rather than the 5th segment where A147T

is found.[18] Similarly, the substituents on the carboxamide nitrogen of PK 11195 interact with Y32 in the first extracellular loop of a crystal structure of the bacterial homolog BcTSPO. Given this moiety interacts with a portion of TSPO distinct from the location of the mutated residue, incorporation of a terminal carboxamide moiety may be useful when designing non-discriminating ligands. An extension from prior work,[19] the structure activity relationships reported herein explore the effect of substitutions of the terminal carboxamide and substitutions at the carbazole 3-position on affinity to both the TSPO isoforms.

RESULTS AND DISCUSSION

Chemistry. The first series of carbazole acetamide ligands were synthesized according to Scheme 1. Intermediate compounds **6a–6f** and **7a** were prepared by NH-deprotonation of 9H-carbazole (**5**) with sodium hydride, followed by the addition of the appropriate alkylating agents (see supporting information for their synthesis). Subsequent *N*-methylation or *N*-ethylation with the appropriate iodoalkane furnished target ligands **7b–7c** and **8a–8f**. An alternative strategy was applied to obtain ligands **11a–11c**, **12a–12c**, **14a** and **15a–15c**. Thus, methyl ester intermediate **9** was hydrolyzed under basic conditions to obtain the carboxylic acid **10**. The carboxylic acid intermediate **10** was then coupled with the appropriate amine to give tertiary amides **11a–11c**, **12a–12c**, **13a–13c** and **14a**. Subsequent catalytic hydrogenation of **13a–13c** with palladium on carbon (Pd/C), followed by acetylation furnished target ligands **15a–15c**. Ligand **14b** was previously reported.[19]

The second series of carbazole acetamide ligands were synthesized in a similar manner starting with 3-bromo-9H-carbazole (**16**), forming key intermediate **17**. Subsequent *N*-methylation or *N*-ethylation with the appropriate iodoalkane furnished target ligands **18a** and **19a**. Utilizing the bromine handle a palladium-catalyzed Suzuki–Miyaura cross-coupling of **18a** and **19a** with the appropriate boronic acid gave target ligands **18b–18c**, **19b–19c** and **20a–20c**.

Scheme 1. Synthesis of carbazole acetamide ligands.[a]

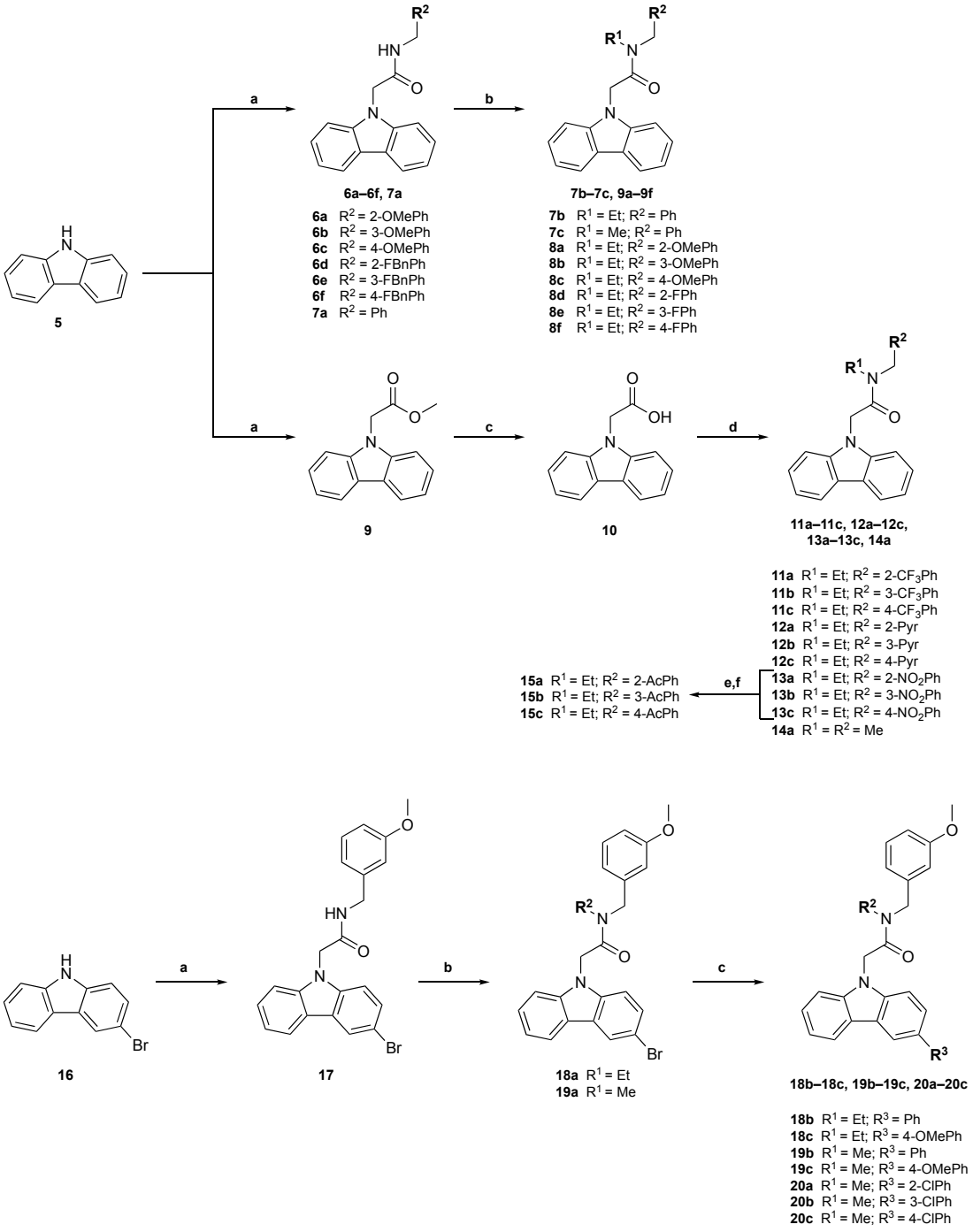

[a]Reagents and Conditions: a) NaH, appropriate alkylating agent, DMF, 0 °C–rt, 2 h, 81–99%; b) KOtBu, DMF, iodoethane or iodomethane, rt, 17 h, 84–93%; c) LiOH, MeOH/H_2O, reflux, 4 h, 72%; d) HBTU, DIPEA, appropriate secondary amine, DMF, rt, 15 h, 68–91%; e) H_2, Pd/C, EtOAc, rt, 6 h, 84–90%; f)

acetic anhydride, CH_2Cl_2, rt, 2 h, 69-76%; g) Cs_2CO_3, $Pd(PPh_3)_4$, appropriate boronic acid, toluene/H_2O, 90 °C, 10 h, 65–77%

Biological Evaluation. The carbazole acetamide TSPO ligands were characterized by competition radioligand binding assays using [^{3}H]PK 11195 on membranes derived from HEK 293 cells overexpressing either A147T or WT TSPO.[19] The binding affinities are expressed as K_i (nM) in Table 1. The binding affinity between TSPO WT and A147T for each ligand is expressed as a ratio (A147T:WT). A ratio between A147T:WT closer to 1 indicates little to no preference between the two TSPO isoforms. The first series of ligands synthesized (**7–8**, **11–12** and **14–15**) encompassed modifications at the R^1 and R^2 position of the amide. This series demonstrates the importance of the disubstituted carboxamide for imparting affinity at both TSPO isoforms. A comparison of ligands **7a–7c,** featuring a phenyl group at the R^2 position, showed complete loss of binding at both TSPO isoforms when R^1 = H (**7a**). Following this, ligand **7c** incorporates a smaller methyl substituent at the R^1 position and showed an improvement in binding affinity at both TSPO A147T (increased 2.4×) and WT (increased 1.3×) forms when compared to ligand **7b** which had an ethyl substituent at R^1. Furthermore, substituting an ethyl group at the R^1 position and a *meta*-methoxyphenyl group at the R^2 position (**8b**) produced good binding affinity at both TSPO isoforms (K_i TSPO WT = 96.1 nM, K_i TSPO A147T = 100.4 nM) and a 1.3x increase in binding affinity at TSPO WT, with respect to ligand **7c**.

Table 1. TSPO binding affinities (K_i) of carbazole acetamide ligands using membranes from TSPO WT and A147T over-expressing HEK 293 cells. Values represent the mean ± SD from at least three independent experiments performed in duplicate.

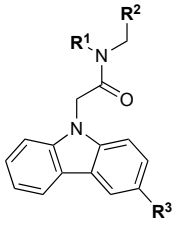

Ligand	R^1	R^2	R^3	TSPO K_i (nM)		A147T: Wild Type
				A147T	Wild Type	
PK 11195				26.7 ± 4.5	22.5 ± 5.2	1.2
7a	H	Ph	H	>10 000	>10 000	N/A
7b	Et	Ph	H	318.5 ± 85.8	70.0 ± 17.8	4.5
7c	Me	Ph	H	132.0 ± 24.0	53.0 ± 17.2	2.5
8a	Et	2-OMePh	H	1551.0 ± 358.1	1531.3 ± 248.8	1.0
8b	Et	3-OMePh	H	100.4 ± 22.5	96.1 ± 30.4	1.0
8c	Et	4-OMePh	H	>10 000	4737.3 ± 447.6	>2.1
8d	Et	2-FPh	H	3123.2 ± 979.4	184.2 ± 55.4	17.0
8e	Et	3-FPh	H	> 10 000	562.5 ± 126.6	>17.8
8f	Et	4-FPh	H	> 10 000	693.8 ± 214.7	> 14.4
11a	Et	2-CF_3Ph	H	>10 000	>10 000	N/A
11b	Et	3-CF_3Ph	H	>10 000	>10 000	N/A
11c	Et	4-CF_3Ph	H	>10 000	>10 000	N/A
12a	Et	2-Pyr	H	>10 000	>10 000	N/A
12b	Et	3-Pyr	H	>10 000	>10 000	N/A
12c	Et	4-Pyr	H	>10 000	>10 000	N/A
14a	Me	Me	H	>10 000	>10 000	N/A
14b	Et	Et	H	176.6 ± 41.6	30.1 ± 3.6	5.9
15a	Et	2-AcPh	H	>10 000	243.0 ± 71.2	>41.2
15b	Et	3-AcPh	H	>10 000	>10 000	N/A
15c	Et	4-AcPh	H	>10 000	>10 000	N/A
18a	Et	3-OMePh	Br	462.3 ± 105.2	468.7 ± 116.9	1.0
18b	Et	3-OMePh	Ph	418.2 ± 18.0	385.3 ± 51.4	1.1
18c	Et	3-OMePh	4-OMePh	369.0 ± 52.9	447.1 ± 74.3	0.8
19a	Me	3-OMePh	Br	>10 000	>10 000	N/A
19b	Me	3-OMePh	Ph	208.4 ± 69.6	231.2 ± 39.3	0.9
19c	Me	3-OMePh	4-OMePh	25.4 ± 8.2	6.6 ± 2.2	3.8
20a	Me	3-OMePh	2-ClPh	214.0 ± 4.4	231.3 ± 16.6	0.9
20b	Me	3-OMePh	3-ClPh	639.4 ± 11.2	200.7 ± 21.5	3.2

20c	Me	3-OMePh	4-ClPh	1696.0 ± 557.9	3555.0 ± 189.3	0.5

Both the *ortho*- (**8a**) and *meta*- (**8b**) substituted methoxyphenyl group exhibited no preference between the two TSPO isoforms. This suggests specific TSPO-drug interactions that are present in both isoforms, resulting in little to no discrimination, which is possibly an important feature in the design of future TSPO ligands. The *para*- (**8c**) position showed significant steric intolerance, as reflected by their micromolar binding affinities. Conversely, maintaining the ethyl group at the R^1 position and incorporating a fluorine (**8d–8f**) substituent on the phenyl group lowered binding affinities to TSPO WT, and abolished all binding at TSPO A147T. The trifluoromethyl (**11a–11c**) or acetamide (**15a–15c**) substituent on the phenyl group at the R^2 position abolished all binding affinity at both TSPO isoforms. Additionally, replacing the phenyl group with a pyridine moiety (**12a–12c**) also produced similar negative effects on affinity. Ligand **14a**, which featured a methyl substituent at both the R^1 and R^2 position showed no binding to the TSPO WT or TSPO A147T. Interestingly, ligand **14b**, featuring an ethyl substituent at both the R^1 and R^2 positions showed improved binding affinities at both TSPO isoforms. A comparison of ligands **14a** and **14b** suggests that larger substituents are more effective at engaging the lipophilic binding sites. Taken together, the binding data from the first series (**7–8**, **11–12** and **14–15**) has shown that ligands **7c** and **8b** were effective at binding TSPO, and ligand **8b** also showed no discrimination between the two TSPO isoforms. In a previous study,[18] substituents at the R^3 position on the carbazole heterocyclic core improved binding affinity. Given this, the next series (**18–20**) was synthesized, featuring a *meta*-methoxyphenyl substituent at the R^2 position, with either an ethyl (**18a–18c**) or methyl (**19a–19c**) substituent at the R^1 position on the carboxamide nitrogen, in conjugation with substituents at the R^3 position on the carbazole heterocyclic core that were chosen based on our previous findings.[18] In agreement with the affinities of the first series, ligands **19a–19c**, containing the methyl substituent at the R^1 position had favorable binding affinities compared to ligands **18a–18c**, containing the ethyl substituent at the R^1 position. Incorporating a *para*-methoxyphenyl group at the R^3 position (**19c**) had the most beneficial effect, with binding affinities

in the low nanomolar range (K_i TSPO WT = 6.6 nM, K_i TSPO A147T = 25.4 nM). Ligand **19c** was shown to have a stronger affinity than the commercially available PK 11195 at both TSPO A147T (increased 1.1×) and WT (increased 3.4×) isoforms. Interestingly, ligands within this subset (**18a–18c**) showed almost identical K_i values, ranging from 369.0–468.7 nM. Following this, ligands **18a–18c** and **19b** also produced little discrimination between the two TSPO isoforms, yielding a A147T:WT ratio of ~1.0, further reinforcing the contribution of an *N*-methoxyphenyl substitution at R^2 to a reduction in binding discrimination between TSPO WT and A147T.

The effect of the PK 11195-inspired chlorophenyl group at the R^3 position on the carbazole was explored. Ligands **20a–20c** were synthesized, whilst maintaining the same carboxamide substituents as ligands **19a–19c** and varying the position of the chlorine substituent on the phenyl group at the R^3 position of the carbazole. Although the data showed no improvement on binding affinity, the K_i values increased at the TSPO WT when the position of the chlorine substituent moved from the *ortho*- (**19a**) to *meta*- (**19b**) to *para*- (**19c**) position on the phenyl group. Interestingly, **19c** and **20c** varied by the substituent at the *para*-position, however they experienced drastic differences in binding affinities at both TSPO isoforms. This finding suggests that the chlorine substituent attached to **20c** could potentially make it sterically unfavorable.

Docking studies were used to investigate the structural basis for the K_i values obtained from biological testing. Ligands **8b**, **19b** and **20a** were chosen on the basis of their similar K_i values for both WT and A147T TSPO and compared to **15a** which showed a stronger K_i for the WT TSPO. Docking and MM-GBSA dG binding scores (obtained by combining molecular mechanics (MM) terms with a generalized Born and surface area (GBSA) solvent mode)[20] are summarized in Table S1 (see supporting information).

Ligands **15a**, **19b** and **20a** all had similar docking scores while a difference of ~3kcal/mol was seen for ligand **8b**. The binding conformation of **8b** was similar for both WT and A147T TSPO, however it was slightly rotated between the two. This could be attributed to greater dispersive interactions between the carbazole ring and THR147 on the A147T TSPO, however the less negative docking score for the A147T

TSPO suggest the formation of these dispersive interactions has a detrimental effect on the overall docking. The MM-GBSA binding scores were similar for each ligand between the WT and A147T TSPO.

Binding poses for ligands **8b** and **15a** are shown in Figure 2, whilst the binding poses for ligands **19b** and **20a** are shown in Figure S1 (see supporting information). **8b**, **19b** and **20a** all exhibited binding poses where the carbazole ring exhibited π-π interactions with TRP95 and also TRP53 in some cases in both WT and A147T TSPO. This pose was also adopted by **15a** in the WT TSPO, while in the A147T TSPO, the ligand has been rotated by 180° and the amine substituents interact with the TRP residues instead. This can be attributed to two factors; the large aromatic substituents attached to the carbazole group in **19b** and **20a** make it sterically unfavorable for the molecule to rotate away from the π-π interactions with TRP95 and TRP53 and the acetanilide substituent on **15a** being able to form interactions with the TRP residues 95, 53 and 143 instead.

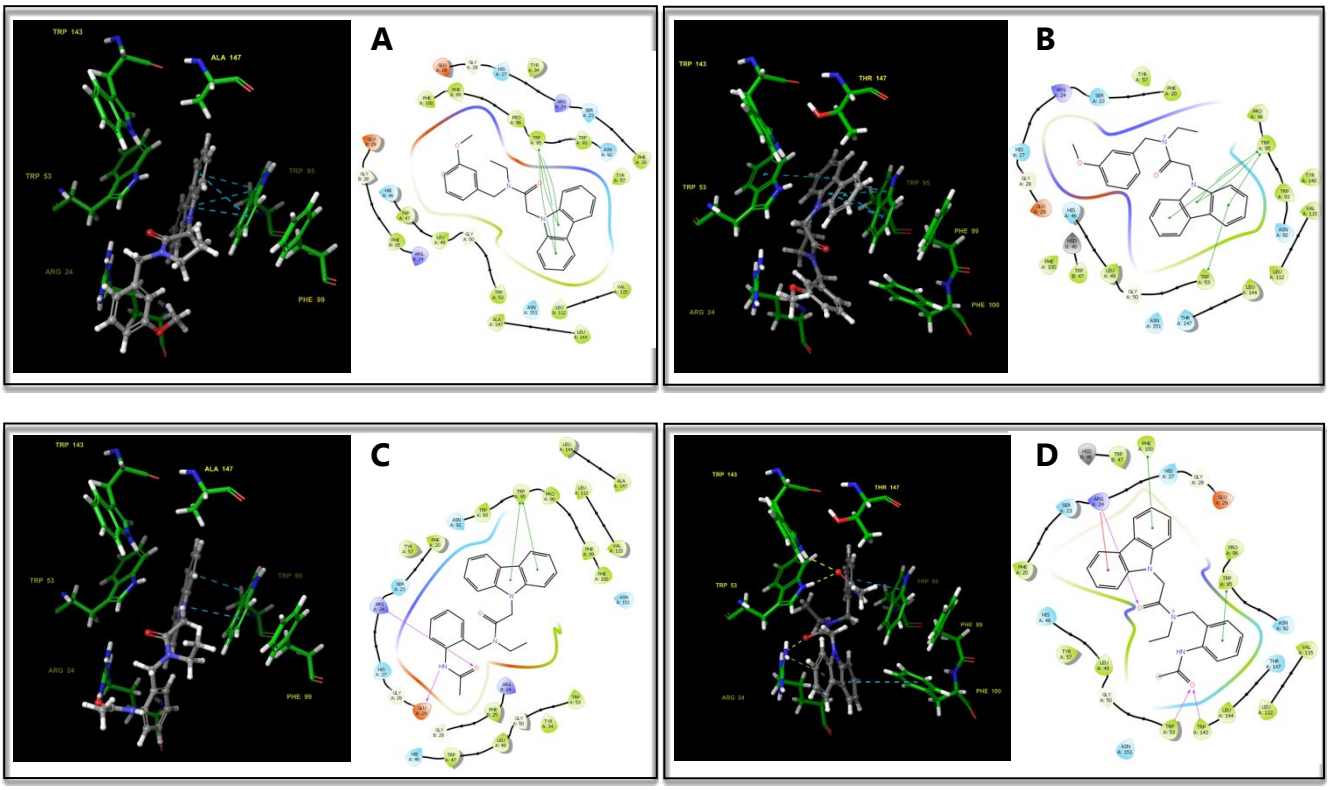

Figure 2. 3-Dimensional and 2-dimensional ligand binding diagrams of the TSPO ligands **8b** and **15a** into the chosen receptors. The crystal structure of the TSPO protein from Bacilus Cereus (PDB ID: 4RYI), was used as the template for homology modelling. (A) Ligand interaction diagram of the ligand **8b** in the wild type TSPO. (B) Ligand interaction diagram of the ligand **8b** in the TSPO A147T. (C) Ligand interaction diagram of the ligand **15a** in the wild type TSPO. (D) Ligand interaction diagram of the ligand **15a** in the TSPO A147T.

TSPO ligands can affect cell viability and proliferation at high concentrations.[19, 21] Given an overall drop-off in binding affinity for TSPO A147T seen in Table 1, a representative subset of TSPO ligands (**7b**, **7c**, **8b**, **18a**, **19c**, **20a**) were investigated for their effect on cell viability and proliferation using HEK 293 cells, to understand whether their biological potency varied according to the different TSPO isoforms.

PK 11195, which has been previously shown to decrease proliferation and viability,[22] was also tested as a positive control. HEK 293 cells that were stably transfected with WT and A147T TSPO were treated with 100 μM of TSPO ligands for 48 h, and cell viability was quantitatively determined using CellTitre

Blue (Figure 3A). The effect on viability of each ligand was measured as a percentage of the viability of vehicle-treated cells. PK 11195 significantly reduced the viability of TSPO WT and A147T cells (65% and 68% respectively) as compared to untreated controls. These results mirror other studies that have showed similar results.[19] All other ligands had no significant effect on the viability of HEK 293 cells. The effect of ligands on cell proliferation was then investigated. Similar to the cell viability assay, 100 μM of TSPO ligands were incubated with HEK 293 cells for 48 h. BrdU ELISA assays were performed as a measurement of cell proliferation and the results were presented as a percentage of vehicle-treated controls (Figure 3B). PK 11195 significantly reduced proliferation in TSPO WT and A147T cells to 83% and 81% of basal proliferation respectively. Out of the eight novel TSPO ligands tested, only **20a** significantly reduced proliferation in both TSPO WT and A147T cell to 89% and 85% respectively. Interestingly, **18b** also attenuated proliferation, but this effect was only seen in A147T cells. From the radioligand binding results (Table 1), **18b** does not discriminate between WT and A147T TSPO in binding (A147T: WT K_i ratio = 1.1), so there is disjunction between the functional data and binding data for this compound.

Recently, TSPO ligands that behave like positive allosteric modulators of the TSPO were reported.[23] The reported TSPO ligands had no effect on proliferation alone, but potentiated the anti-proliferative effect of PK 11195. Given the lack of functional activity of most of the novel TSPO ligands, TSPO WT and A147T cells were co-treated with both PK 11195 (100 μM) and the novel ligands (100 μM, Figure 3C) in order to examine whether the TSPO ligands showed any positive allosteric modulator-like activity. **19b** decreased proliferation when co-treated with PK 11195, compared to when treated with PK 11195 alone. This effect was observed in both TSPO WT and A147T. Although only a small effect at a high concentration, this suggests **19b** may be able to potentiate the effect of PK 11195 in reducing cell proliferation.

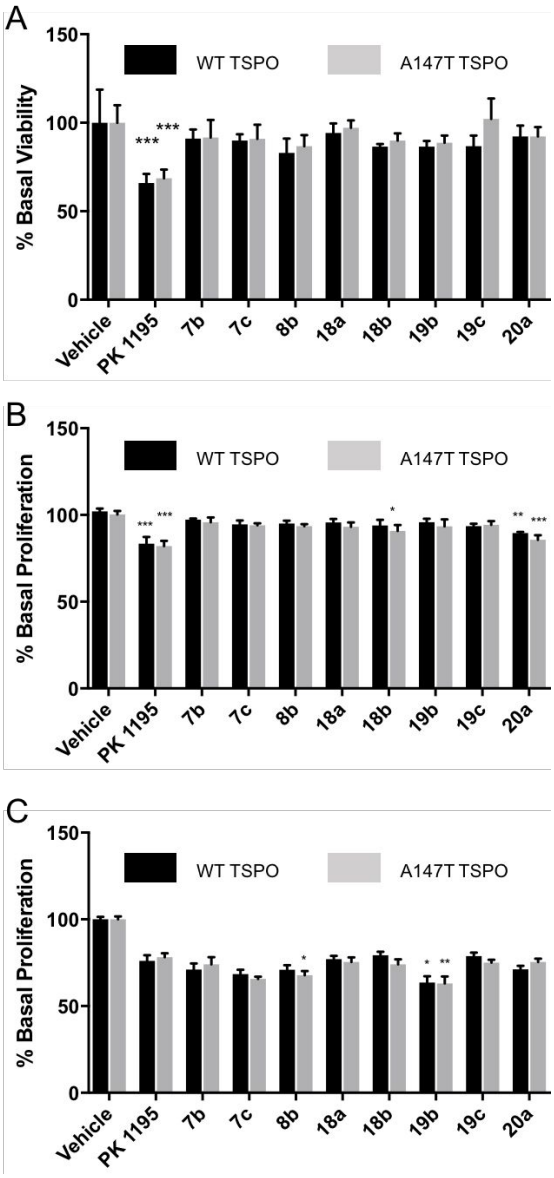

Figure 3. Cell viability and proliferation of HEK 293 cells overexpressing TSPO WT and TSPO A147T after treatment with novel TSPO ligands. (A) Cell viability was determined using CellTitre Blue. Both cell lines were treated with 100 μM of the TSPO ligands for 48 hours and were then incubated with CellTitre Blue for 4 hours. Cell proliferation was assessed with a BrdU ELISA assay. Both cell lines were treated with novel TSPO ligands in the absence (B) or presence of (C) PK 11195 for 48 hours. Data are expressed as mean ± SD ($n \geq 3$, two-way ANOVA followed by Dunnett's multiple comparison test, *$p < 0.05$, **$p < 0.01$, ***$p < 0.001$, with (A) and (B) compared with vehicle-treated cells and (C) compared to PK 11195).

Changes in neurosteroid levels have been reported in psychiatric disorders such as anxiety disorder.[24] Translocation of cholesterol through the mitochondrial membrane is a rate-limiting step in the production of neurosteroids such as allopregnanolone.[25] At least *in vitro*, TSPO mediates this translocation of cholesterol,[24] and consequently, TSPO ligands administered to rodents exert anxiolytic effects by increasing the release of pregnenolone.[26-27] Therefore, the steroidogenic activity of the TSPO ligands was investigated by measuring the release of pregnenolone from C6 glioma cells using ELISA. As expected from previous studies, PK 11195 significantly increased pregnenolone release in C6 cells.[28] In contrast, two high affinity ligands reported in this paper, **8b** and **19c**, showed no significant steroidogenic effects.

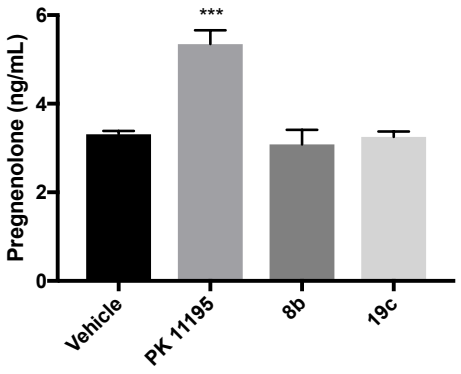

Figure 4. Effects of TSPO ligands (PK 11195, **8b** and **19c**) on C6 glioma steroidogenesis. Pregnenolone ELISA assays were performed as a measurement of pregnenolone release. 100 μM of the TSPO ligands were incubated in ELISA buffer for 2 hours. PK 11195 significantly increased pregnenolone release, and no change was observed for **8b** and **19c** compared to vehicle-treated control. Values represent mean ± SD ($n \geq 3$, one-way ANOVA followed by Dunnett's multiple comparison test, *** $p < 0.001$ compared to vehicle-treated cells).

Given that binding affinity was measured on cell membranes, yet functional activity was measured on intact cells, and the high affinity ligands did not result in potent functional activity; we ascertained whether

the ligands were able to cross the cell membrane and reach TSPO in the mitochondria of intact cells. Whole cell radioligand binding experiments were performed with PK 11195 and two novel ligands **8b** and **19c** that showed the highest membrane binding affinities.

The binding affinities determined by whole cell radioligand binding (Table 2) mirrored the binding affinities obtained from competition radioligand binding using membranes (Table 1). This suggests that the novel ligands can cross the cell membrane and reach the mitochondrial TSPO target. Given most of the novel ligands had little to no effect on the viability or proliferation of cells when administered by themselves, and high affinity ligands could cross the cell membrane, the binding sensitivity for TSPO appears to have no correlation to its anti-proliferative, cytotoxic and steroidogenic function for these ligands. This suggests other factors govern the functional capacity of TSPO ligands, which is supported by recent work showing the importance of residence time to cytotoxic and steroidogenic functional efficacy.[24]

Table 2. Binding affinities of three TSPO ligands using whole cell radioligand binding. Values represent the mean ± SD from at least three independent experiments performed in duplicate.

Ligand	TSPO K_i (nM)		A147T: Wild Type
	A147T	Wild Type	
PK 11195	31.5 ± 7.5	13.6 ± 3.4	2.3
8b	277.0 ± 77.9	217.3 ± 0.6	1.2
19c	23.2 ± 7.3	3.2 ± 0.6	7.3

CONCLUSIONS

A novel series of carbazole acetamide ligands were synthesized and shown to be WT and A147T TSPO ligands. In general, ligands with a *N*-methoxyphenyl substitution at R^2 show a reduction in binding discrimination between TSPO WT and A147T. In particular, the *N*-(3-methoxybenzyl)-*N*-ethyl (**8b**) substitution binds with similarly high affinity to both TSPO WT and A147T. In addition, the *para*-methoxyphenyl substitution at the 3-position of the carbazole scaffold dramatically improved the K_i value to the low nanomolar range.

A subset of high binding affinity ligands (**7b**, **7c**, **8b**, **18a**, **19c**, **20a**) were tested *in vitro* to determine their ability to reduce cell viability and proliferation in HEK 293 cells transfected with WT and A147T TSPO. Only **20a** significantly reduced cell proliferation, all other ligands had no effect on cell viability despite showing affinity for TSPO. The steroidogenic activity of the TSPO ligands **8b** and **19c** was investigated *in vitro* by measuring the release of pregnenolone from C6 glioma and showed no significant steroidogenic effects.

These novel insights will aid in the further development of TSPO ligands for therapeutic and diagnostic imaging in neuroinflammation using PET.

EXPERIMENTAL SECTION

General Procedures. Unless otherwise stated, all solvents and reagents were purchased and used from commercial sources. Anhydrous solvents were obtained from an Innovative Technology PureSolv7 purification system. Tetrahydrofuran and dichloromethane were dried through an alumina column. *N,N*-Dimethylformamide was dried through a 5 Å molecular sieve column. All reagents were weighed out under ambient conditions. All reactions were performed under nitrogen or argon, unless otherwise stated. Melting points using an Optimelt Automated melting point apparatus from Stanford Research Systems were measured in open capillary tubes. IR spectra were recorded neat using a Bruker ALPHA FT-IR spectrometer and peaks are expressed in wavenumbers (cm^{-1}). Nuclear magnetic resonance spectra were

recorded on Bruker Advance DRX 300 or Bruker Advance DRX 400 Ascend spectrometers at 300 or 400 MHz ^{1}H NMR frequency, 75 or 101 MHz ^{13}C NMR frequency and 282 MHz ^{19}F NMR frequency. H, C and F chemical shifts are expressed as parts per million (ppm). All resonances are reported as chemical shift (δ) and are referenced to the solvent residual peak. Multiplicities are reported as follows: s (singlet), br (broad), d (doublet), dd (doublet of doublets), t (triplet), q (quartet) and m (multiplet). Coupling constants (*J*) are reported in Hz. Elemental microanalysis was obtained from the School of Human Sciences at London Metropolitan University, England. Low- and high-resolution mass spectra were obtained through electron ionization (ESI). Low-resolution mass spectra were performed on a Finnigan LCQ mass spectrometer. High-resolution mass spectra were performed on a Bruker 7T Apex Qe Fourier Transform Ion Cyclotron resonance mass spectrometer equipped with an Apollo II ESI/APCI/MALDI Dual source. High performance liquid chromatography (HPLC) was performed on the Waters Alliance 2695 apparatus equipped with Waters 2996 photodiode array detector, set at 254 nm. Separation using a SunFireTM C18 column (5 μm, 2.1 x 150 mm) was achieved using water (solvent A) and acetonitrile (solvent B) at a flow rate of 0.2 mL/min. The method consisted of 0% B to 100% B over 30 minutes. HPLC data is recorded as percentage purity and retention time (RT) in minutes. Purity of all final compounds was 95% or higher.

Materials. Non-commercially available alkylating agents and secondary amines have been prepared according to known procedures (see supporting information).

General Procedure for the Synthesis of 6a–6f, 7a, 9 and 17. Sodium hydride (60% w/w dispersion in mineral oil, 1.5 equiv.) was added portion-wise to a solution of the appropriate aromatic amines (1.0 equiv.) in tetrahydrofuran (0.2 M) at 0 °C. The reaction mixture was warmed to ambient temperature and stirred for 30 minutes before being cooled back down to 0 °C. The appropriate alkylating agent (1.0 equiv.) was added dropwise at 0 °C. The reaction mixture was warmed to ambient temperature and stirred for an additional 2 hours. The reaction mixture was poured into ice-cold water and neutralized with aqueous hydrochloric acid (1 M). The organic layer was collected and the aqueous layer was extracted with ethyl

acetate (3×). The organic extracts were combined, dried over anhydrous magnesium sulfate and concentrated *in vacuo*. Unless otherwise specified, purification was achieved by trituration using diethyl ether gave the desired product (266 mg, 0.772 mmol, 98%) as a colorless powder.

General Procedure for the Synthesis of 7b–7c, 8a–8f, 18a and 19a. Potassium *tert*-butoxide (2.0 equiv.) was added portion-wise to a solution of the appropriate secondary amide (1.0 equiv.) in tetrahydrofuran (0.3 M). The reaction mixture was then stirred for 30 minutes at ambient temperature. The appropriate iodoalkane (1.5 equiv.) was added dropwise at 0 °C and the mixture was then warmed to ambient temperature and stirred for 17 hours. The reaction mixture was neutralized with aqueous hydrochloric acid (1 M). The organic layer was collected and the aqueous layer was extracted with ethyl acetate (3×). The organic layers were combined, dried over anhydrous magnesium sulfate and concentrated *in vacuo*. The ^{1}H NMR spectrum of this amide shows the presence of two different rotamers in a 1:1 ratio. For the sake of simplicity, the NMR data for only one rotamer are reported.

General Procedure for the Synthesis of 11a–11c, 12a–12c, 13a–13c, 14a. To a solution of the carboxylic acid **10** (100 mg, 0.444 mmol, 1.0 equiv.), HBTU (253 mg, 0.666 mmol, 1.5 equiv.) and the appropriate secondary amine (1.0 equiv.) in anhydrous dimethylformamide (0.2 M) was added *N,N*-diisopropylethylamine (150 μL, 0.888 mmol, 2.0 equiv.). The mixture was stirred at ambient temperature for 15 hours. Upon completion, water was added and the aqueous mixture was extracted with ethyl acetate (3×). The mixture was washed with an aqueous solution of saturated sodium bicarbonate (1×), hydrochloric acid (1×, 2 M), water (2×) and brine (1×). The organic extract was then dried over anhydrous magnesium sulfate and concentrated *in vacuo.*

General Procedure for the Synthesis of 15a–15c. To a mixture of the appropriate aryl nitro compounds (100 mg, 0.258 mmol, 1.0 equiv.) in ethyl acetate (5 mL) was added palladium on carbon (10 mg, 10 wt%). The reaction mixture degassed under nitrogen for 5 minutes and then stirred at ambient temperature for 6 hours under a hydrogen atmosphere (1 atm). The mixture was filtered through a pad of Celite® and the pad washed with ethyl acetate. The filtrate was concentrated *in vacuo* to give the crude

residue. The product was carried on to the next step without purification. To a mixture of the crude product in dichloromethane (2 mL) was added acetic anhydride (30 μL, 0.318 mmol, 1.1 equiv.) dropwise. The reaction mixture was stirred at ambient temperature for 2 hours, then poured into an aqueous solution of saturated sodium bicarbonate (2 mL). The aqueous phase was extracted with dichloromethane (3×5 mL). The organic layers were combined, dried over anhydrous magnesium sulfate and concentrated *in vacuo*. Purification was achieved by flashchromatography (ethyl acetate/hexane, 3:7 v/v) on silica gel.

General Procedure for the Synthesis of 18b–18c, 19b–19c and 20a–20c. A suspension of **18a** or **19a** (1.0 equiv.), appropriate phenylboronic acid (1.5 equiv.), and caesium carbonate (2.5 equiv.) in toluene/water (0.1 M, 3:1 v/v) was degassed under argon for 10 minutes. $Pd(dppf)Cl_2$ (5 mol%) was added under argon. The reaction mixture was heated to 80 °C and stirred for 10 hours. Upon completion, the reaction mixture was cooled to ambient temperature and evaporated to dryness. This crude residue was purified by flash column chromatography (ethyl acetate/hexane, 3:7 v/v) on silica gel.

2-(9*H*-Carbazol-9-yl)-*N*-(2-methoxybenzyl)acetamide (6a). White solid; yield 98% (266 mg, 0.772 mmol). $\mathbf{R_f}$ 0.59 (ethyl acetate/hexane, 3:7 v/v); **mp** 207–209 °C; **^{1}H NMR (300 MHz, DMSO) δ =** 8.61 (t, *J* = 5.8 Hz, 1H, N**H**), 8.18 – 8.15 (m, 2H, Ar**H**), 7.59 – 7.56 (m, 2H, Ar**H**), 7.47 – 7.42 (m, 2H, Ar**H**), 7.28 – 7.19 (m, 4H, Ar**H**), 6.99 – 6.84 (m, 2H, Ar**H**), 5.13 (s, 2H, C$\mathbf{H_2}$CO), 4.28 (d, *J* = 5.7 Hz, 2H, NHC$\mathbf{H_2}$), 3.77 (s, 3H, OC$\mathbf{H_3}$); **^{13}C NMR (75 MHz, DMSO) δ =** 167.45 (**C**O), 156.65 (Ar), 140.58 (2×Ar), 128.18 (Ar), 127.94 (Ar), 126.28 (2×Ar), 125.59 (Ar), 122.21 (2×Ar), 120.10 (Ar), 120.03 (2×Ar), 118.95 (2×Ar), 110.44 (Ar), 109.35 (2×Ar), 55.24 (O**C**H_3), 45.49 (**C**H_2CO), 37.50 (NH**C**H_2); **LRMS (+ESI)** 367 [$(M + Na)^+$ 100%]; **HRMS (+ESI)** Calcd for $C_{22}H_{20}N_2O_2$ ($[M + Na]^+$ 367.1417. Found: 367.1419; **IR (vmax/cm^{-1})** 3284, 2991, 1648, 1488, 1230, 1154, 1123, 1051, 745, 718, 423.

2-(9*H*-Carbazol-9-yl)-*N*-(3-methoxybenzyl)acetamide (6b). White solid; yield 98% (262 mg, 0.761 mmol). $\mathbf{R_f}$ 0.53 (ethyl acetate/hexane, 3:7 v/v); **mp** 198–200 °C; **^{1}H NMR (300 MHz, DMSO) δ =** 8.11 – 8.08 (m, 2H, Ar**H**), 7.52 – 7.46 (m, 2H, Ar**H**), 7.39 – 7.36 (m, 2H, Ar**H**) 7.32 – 7.25 (m, 2H, Ar**H**), 7.11 – 7.06 (m, 1H, Ar**H**), 6.71 – 6.50 (m, 3H, Ar**H**), 5.91 (t, *J* = 5.8 Hz, 1H, N**H**), 4.97 (s, 2H, C$\mathbf{H_2}$CO), 4.34

(d, J = 5.8 Hz, 2H, NHC**H**$_2$), 3.63 (s, 3H, OC**H**$_3$); **^{13}C NMR (75 MHz, DMSO) δ** = 168.07 (**C**O), 159.75 (Ar), 140.26 (2×Ar), 138.90 (Ar), 129.58 (Ar), 126.52 (2×Ar), 123.48 (2×Ar), 120.70 (Ar), 120.42 (2×Ar), 119.32 (2×Ar), 113.32 (Ar), 112.12 (Ar), 108.54 (2×Ar), 55.10 (O**C**H$_3$), 47.16 (**C**H$_2$CO), 43.07 (NH**C**H$_2$); **LRMS (+ESI)** 367 [(M + Na)$^+$ 100%]; **HRMS (+ESI)** Calcd for $C_{22}H_{20}N_2O_2$ ([M + Na]$^+$ 367.1417. Found: 367.1410; **IR (vmax/cm^{-1})** 3669, 2985, 2212, 1649, 1066, 483.

2-(9*H*-Carbazol-9-yl)-*N*-(4-methoxybenzyl)acetamide (6c). White solid; yield 99% (266 mg, 0.772 mmol). **R$_f$** 0.40 (ethyl acetate/hexane, 3:7 v/v); **mp** 210–212 °C; **^{1}H NMR (300 MHz, DMSO) δ** = 8.73 (t, J = 5.8 Hz, 1H, N**H**), 8.20 – 8.10 (m, 2H, Ar**H**), 7.55 – 7.50 (m, 2H, Ar**H**), 7.47 – 7.38 (m, 2H, Ar**H**), 7.24 – 7.13 (m, 4H Ar**H**), 6.91 – 6.86 (m, 2H, Ar**H**), 5.08 (s, 2H, C**H$_2$**CO), 4.25 (d, J = 5.8 Hz, 2H, NHC**H$_2$**), 3.74 (s, 3H, OC**H$_3$**); **^{13}C NMR (75 MHz, DMSO) δ** = 167.31 (**C**O), 158.23 (Ar), 140.59 (2×Ar), 130.97 (Ar), 128.61 (2×Ar), 125.59 (2×Ar), 122.22 (2×Ar), 120.11 (2×Ar), 118.95 (2×Ar), 113.64 (2×Ar), 109.30 (2×Ar), 55.04 (O**C**H$_3$), 45.55 (**C**H$_2$CO), 41.71 (NH**C**H$_2$); **LRMS (+ESI)** 367 [(M + Na)$^+$ 100%]; **HRMS (+ESI)** Calcd for $C_{22}H_{20}N_2O_2$ ([M + Na]$^+$ 367.1417. Found: 367.1416; **IR (vmax/cm^{-1})** 3293, 2991, 1649, 1489, 1237, 1154, 1122, 746, 718, 528.

2-(9*H*-Carbazol-9-yl)-*N*-(2-fluorobenzyl)acetamide (6d). White solid; yield 88% (238 mg, 0.716 mmol). **R$_f$** 0.53 (ethyl acetate/hexane, 3:7 v/v); **mp** 202–204 °C; **^{1}H NMR (300 MHz, DMSO) δ** = 8.15 – 7.99 (m, 2H, Ar**H**), 7.53 – 6.83 (m, 10H, Ar**H**), 5.95 (t, J = 6.1 Hz, 1H, N**H**), 4.94 (s, 2H, C**H$_2$**CO), 4.39 (d, J = 6.1 Hz, 2H, NHC**H$_2$**); **^{13}C NMR (75 MHz, DMSO) δ** = 168.15 (**C**O), 162.39 (d, J = 245.8 Hz, Ar), 140.27 (2×Ar), 129.39 (d, J = 6.1 Hz, Ar), 129.15 (d, J = 8.2 Hz, Ar), 126.47 (2×Ar), 125.32 (d, J = 8.2 Hz, Ar), 124.02 (d, J = 3.4 Hz, Ar), 123.50 (2×Ar), 120.47 (2×Ar), 120.19 (2×Ar), 114.55 (d, J = 21.6 Hz, Ar), 108.56 (2×Ar), 47.16 (**C**H$_2$CO), 37.29 (NH**C**H$_2$); **^{19}F NMR (282 MHz, DMSO) δ** = –117.87 (Ar**F**); **LRMS (+ESI)** 355 [(M + Na)$^+$ 100%]; **HRMS (+ESI)** Calcd for $C_{21}H_{17}FN_2O$ ([M + Na]$^+$ 355.1217. Found: 355.1220; **IR (vmax/cm^{-1})** 2998, 2201, 1654, 1455, 1211, 1074, 809, 716, 461.

2-(9*H*-Carbazol-9-yl)-*N*-(3-fluorobenzyl)acetamide (6e). White solid; yield 86% (233 mg, 0.701 mmol). **R$_f$** 0.47 (ethyl acetate/hexane, 3:7 v/v); **mp** 186–188 °C; **^{1}H NMR (300 MHz, DMSO) δ** = 8.14

(d, *J* = 7.5 Hz, 2H, Ar**H**), 7.50 – 7.37 (m, 4H, Ar**H**), 7.32 – 7.28 (m, 3H, Ar**H**), 7.20 – 7.11 (m, 3H, Ar**H**), 5.91 (t, *J* = 6.2 Hz, 1H, N**H**), 4.99 (s, 2H, C**H**$_2$CO), 4.34 (d, *J* = 6.2 Hz, 2H, NHC**H**$_2$); **^{13}C NMR (75 MHz, DMSO) δ =** 168.18 (**C**O), 159.56 (d, *J* = 252.6 Hz, Ar), 140.20 (2×Ar), 134.85 (d, *J* = 3.6 Hz, Ar), 130.74 (d, *J* = 8.2 Hz, Ar), 127.46 (2×Ar), 125.32 (d, *J* = 4.2 Hz, Ar), 124.03 (2×Ar), 120.55 (2×Ar), 120.19 (2×Ar), 115.47 (d, *J* = 20.2 Hz, Ar), 114.56 (d, *J* = 21.4 Hz, Ar), 108.89 (2×Ar), 47.15 (**C**H$_2$CO), 42.41 (NH**C**H$_2$); **^{19}F NMR (282 MHz, DMSO) δ =** –115.84 (Ar**F**); **LRMS (+ESI)** 355 [(M + Na)$^+$ 100%]; **HRMS (+ESI)** Calcd for $C_{21}H_{17}FN_2O$ ([M + Na]$^+$ 355.1217. Found: 355.1218; **IR (νmax/cm^{-1})** 3256, 2962, 1648, 1451, 1327, 1206, 745, 718, 421.

2-(9*H*-Carbazol-9-yl)-*N*-(4-fluorobenzyl)acetamide (6f). White solid; yield 88% (238 mg, 0.716 mmol). **R$_f$** 0.40 (ethyl acetate/hexane, 3:7 v/v); **mp** 227–229 °C; **^{1}H NMR (300 MHz, DMSO) δ =** 8.10 (d, *J* = 7.7 Hz, 2H, Ar**H**), 7.49 (t, *J* = 7.7 Hz, 2H, Ar**H**), 7.35 – 7.21 (m, 4H, Ar**H**), 6.96 (dd, *J* = 8.5 Hz, 5.4 Hz, 2H, Ar**H**), 6.85 (t, *J* = 8.5 Hz, 2H, Ar**H**), 5.89 (t, *J* = 6.1 Hz, 1H, N**H**), 4.95 (s, 2H, C**H**$_2$CO), 4.30 (d, *J* = 6.1 Hz, 2H, NHC**H**$_2$); **^{13}C NMR (75 MHz, DMSO) δ =** 168.08 (**C**O), 160.23 (d, *J* = 251.3 Hz, Ar) 140.23 (2×Ar), 133.24 (d, *J* = 3.2 Hz, Ar), 128.92 (d, *J* = 8.1 Hz, 2×Ar), 126.51 (2×Ar), 123.49 (2×Ar), 120.70 (2×Ar), 120.46 (2×Ar), 115.25 (d, *J* = 21.8 Hz, 2×Ar), 108.54 (2×Ar), 47.15 (**C**H$_2$CO), 42.41 (NH**C**H$_2$); **^{19}F NMR (282 MHz, DMSO) δ =** –115.33 (Ar**F**); **LRMS (+ESI)** 355 [(M + Na)$^+$ 100%]; **HRMS (+ESI)** Calcd for $C_{21}H_{17}FN_2O$ ([M + Na]$^+$ 355.1217. Found: 355.1220; **IR (νmax/cm^{-1})** 3262, 2854, 2011, 1649, 1462, 1218, 833, 750, 449.

***N*-Benzyl-*2-(9H*-carbazol-9-yl)acetamide (7a).** White solid; yield 86% (238 mg, 0.757 mmol). **R$_f$** 0.47 (ethyl acetate/hexane, 3:7 v/v); **mp** 226–228 °C; **^{1}H NMR (300 MHz, CDCl$_3$) δ** = 8.11 – 8.09 (m, 2H, Ar**H**), 7.52 – 7.47 (m, 2H, Ar**H**), 7.38 – 7.25 (m, 4H, Ar**H**), 7.19 – 7.15 (m, 3H, Ar**H**), 7.01 – 6.98 (m, 2H, Ar**H**), 5.90 (s, 1H, N**H**), 4.99 (s, 2H, C**H**$_2$CO), 4.37 (d, *J* = 6.1, 2H, NHC**H**$_2$); **^{13}C NMR (75 MHz, CDCl$_3$) δ =** 168.07 (**C**O), 140.27 (2×Ar), 137.38 (Ar), 128.54 (2×Ar), 127.39 (2×Ar), 127.11 (Ar), 126.49 (2×Ar), 123.50 (2×Ar), 120.67 (2×Ar), 120.42 (2×Ar), 108.58 (2×Ar), 47.21 (**C**H$_2$CO), 43.11

(NH**C**H_2); **LRMS (+ESI)** 337 [(M + Na)$^+$ 100%]; **IR (vmax/cm^{-1})** 3675, 2987, 2900, 1394, 1250, 1066, 892, 444; Found: C, 80.16; H, 5.81; N, 8.92. Calc for $C_{21}H_{18}N_2O$: C, 80.23; H, 5.77; N, 8.91%

***N*-Benzyl-2-(9*H*-carbazol-9-yl)-*N*-ethylacetamide (7b).** White solid; yield 90% (98 mg, 0.286 mmol). **R$_f$** 0.65 (ethyl acetate/hexane, 3:7 v/v); **mp** 143–145 °C; **^{1}H NMR (300 MHz; CDCl$_3$) δ =** 8.06 (d, *J* = 7.8 Hz, 2H, Ar**H**), 7.46 – 7.16 (m, 11H, Ar**H**), 5.12 (s, 2H, C**H$_2$**CO), 4.62 (s, 2H, C**H$_2$**Ph), 3.35 (q, *J* = 7.3 Hz, 2H, C**H$_2$**CH$_3$), 1.04 (t, *J* = 7.3 Hz, 3H, CH$_2$C**H$_3$**); **^{13}C NMR (75 MHz, CDCl$_3$) δ =** 166.19 (**C**O), 140.75 (2×Ar), 139.95 (Ar), 128.52 (2×Ar), 127.38 (2×Ar), 127.11 (Ar), 126.49 (2×Ar), 123.50 (2×Ar), 120.67 (2×Ar), 120.42 (2×Ar), 108.46 (2×Ar), 49.83 (**C**H$_2$CO), 48.67 (**C**H$_2$Ph), 43.11 (**C**H$_2$CH$_3$), 13.25 (CH$_2$**C**H$_3$); **LRMS (+ESI)** 365 [(M + Na)$^+$ 40%], 343 [(M + H)$^+$ 100%]; **IR (vmax/cm^{-1})** 3402, 1658, 1536, 1452, 799; Found: C, 80.55; H, 6.49; N, 8.19. Calc for $C_{23}H_{22}N_2O$: C, 80.67; H, 6.48; N, 8.18%

***N*-Benzyl-2-(9*H*-carbazol-9-yl)-*N*-methylacetamide (7c).** White solid; yield 87% (91 mg, 0.277 mmol). **R$_f$** 0.57 (ethyl acetate/hexane, 3:7 v/v); **mp** 139–141 °C; **^{1}H NMR (300 MHz; CDCl$_3$) δ =** 8.07 (d, *J* = 7.7 Hz, 2H, Ar**H**), 7.46 – 7.11 (m, 11H, Ar**H**), 4.97 (s, 2H, C**H$_2$**CO), 4.56 (s, 2H, C**H$_2$**Ph), 2.88 (s, 3H, C**H$_3$**); **^{13}C NMR (75 MHz, CDCl$_3$) δ =** 167.70 (**C**O), 140.79 (2×Ar), 136.75 (Ar), 128.68 (2×Ar), 127.89 (2×Ar), 127.60 (Ar), 125.94 (2×Ar), 123.22 (2×Ar), 120.46 (2×Ar), 119.51 (2×Ar), 108.58 (2×Ar), 51.61 (C**H$_2$**CO), 45.58 (**C**H$_2$Ph), 34.21 (**C**H$_3$); **LRMS (+ESI)** 351 [(M + Na)$^+$ 100%]; **IR (vmax/cm^{-1})** 3674, 2986, 1649, 1406, 1218, 1067, 745, 717, 420; Found: C, 80.52; H, 6.10; N, 8.42. Calc for $C_{22}H_{20}N_2O$: C, 80.46; H, 6.14; N, 8.53%

2-(9*H*-Carbazol-9-yl)-*N*-ethyl-*N*-(2-methoxybenzyl)acetamide (8a). White solid; yield 88% (190 mg, 0.510 mmol). **R$_f$** 0.65 (ethyl acetate/hexane, 3:7 v/v); **mp** 135–137 °C; **^{1}H NMR (300 MHz, CDCl$_3$) δ** = 8.09 – 8.07 (m, 2H, Ar**H**), 7.43 – 7.29 (m, 3H, Ar**H**), 7.25 – 7.10 (m, 5H, Ar**H**), 6.99 – 6.82 (m, 2H, Ar**H**), 5.03 (s, 2H, C**H$_2$**Ph), 4.57 (s, 2H, C**H$_2$**CO), 3.85 (s, 3H, OC**H$_3$**), 3.46 (q, *J* = 7.1 Hz, 2H, C**H$_2$**CH$_3$), 1.10 (t, *J* = 7.1 Hz, 3H, CH$_2$C**H$_3$**); **^{13}C NMR (75 MHz, CDCl$_3$) δ** = 167.34 (**C**O), 157.04 (Ar), 140.88 (2×Ar), 129.03 (2×Ar), 126.97 (Ar), 125.74 (2×Ar), 124.28 (Ar), 123.18 (2×Ar), 120.73 (Ar), 120.29 (2×Ar), 119.22 (2×Ar), 108.57 (2×Ar), 55.30 (OC**H$_3$**), 45.99 (C**H$_2$**CO), 45.35 (C**H$_2$**Ph), 41.66 (C**H$_2$**CH$_3$),

12.70 (CH_2CH_3); **LRMS (+ESI)** 395 [$(M + Na)^+$ 100%]; **IR (νmax/cm^{-1})** 2992, 1650, 1489, 1237, 1154, 1072, 745, 718, 529; **HPLC** τ_R = 29.83 min (98.0% purity); Found: C, 77.38; H, 6.55; N, 7.48. Calc for $C_{24}H_{24}N_2O_2$: C, 77.39; H, 6.50; N, 7.52%

2-(9*H*-Carbazol-9-yl)-*N*-ethyl-*N*-(3-methoxybenzyl)acetamide (8b). White solid; yield 93% (201 mg, 0.540 mmol). **R_f** 0.45 (ethyl acetate/hexane, 3:7 v/v); **mp** 46–48 °C; **^{1}H NMR (300 MHz, $CDCl_3$) δ** = 8.03 – 7.94 (m, 2H, Ar**H**), 7.40 – 7.26 (m, 3H, Ar**H**), 7.20 – 7.10 (m, 4H, Ar**H**), 6.78 – 6.57 (m, 3H, Ar**H**), 5.02 (s, 2H, C$\mathbf{H}_2$CO), 4.51 (s, 2H, C$\mathbf{H}_2$Ph), 3.65 (s, 3H, OC$\mathbf{H}_3$), 3.27 (q, *J* = 7.1 Hz, 2H, C$\mathbf{H}_2$CH$_3$), 0.99 (t, *J* = 7.1 Hz, 3H, CH$_2$C$\mathbf{H}_3$); **^{13}C NMR (75 MHz, $CDCl_3$) δ** = 167.36 (**C**O), 159.90 (Ar), 140.76 (2×Ar), 130.16 (Ar), 129.56 (Ar), 125.93 (2×Ar), 123.24 (2×Ar), 120.48 (2×Ar), 119.48 (2×Ar), 118.09 (Ar), 113.32 (Ar), 113.14 (Ar) 108.48 (2×Ar), 55.20 (O**C**H$_3$), 45.64 (**C**H$_2$CO), 45.40 (**C**H$_2$Ph), 41.16 (**C**H$_2$CH$_3$), 13.62 (CH$_2$**C**H$_3$); **LRMS (+ESI)** 395 [$(M + Na)^+$ 100%]; **IR (νmax/cm^{-1})** 2967, 1643, 1486, 1242, 747, 719, 512; Found: C, 77.38; H, 6.59; N, 7.40. Calc for $C_{24}H_{24}N_2O_2$: C, 77.39; H, 6.50; N, 7.52%

2-(9*H*-Carbazol-9-yl)-*N*-ethyl-*N*-(4-methoxybenzyl)acetamide (8c). White solid; yield 91% (197 mg, 0.529 mmol). **R_f** 0.50 (ethyl acetate/hexane, 3:7 v/v); **mp** 119–121 °C; **^{1}H NMR (300 MHz, $CDCl_3$) δ** = 8.08 – 8.00 (m, 2H, Ar**H**), 7.44 – 7.34 (m, 2H, Ar**H**), 7.27 – 7.02 (m, 6H, Ar**H**), 6.88 – 6.78 (m, 2H, Ar**H**), 4.93 (s, 2H, C$\mathbf{H}_2$CO), 4.45 (s, 2H, NHC$\mathbf{H}_2$), 3.78 (s, 3H, OC$\mathbf{H}_3$), 3.24 (q, *J* = 7.1 Hz, 2H, C$\mathbf{H}_2$CH$_3$), 1.05 (t, *J* = 7.1 Hz, 3H, CH$_2$C$\mathbf{H}_3$); **^{13}C NMR (75 MHz, $CDCl_3$) δ** = 167.15 (**C**O), 159.23 (Ar), 140.81 (2×Ar), 129.71 (2×Ar), 128.27 (Ar), 125.91 (2×Ar), 123.17 (2×Ar), 120.42 (2×Ar), 119.42 (2×Ar), 114.47 (2×Ar), 108.57 (2×Ar), 55.43 (O**C**H$_3$), 49.52 (**C**H$_2$CO), 47.79 (**C**H$_2$Ph), 45.16 (**C**H$_2$CH$_3$), 13.66 (CH$_2$**C**H$_3$); **LRMS (+ESI)** 395 [$(M + Na)^+$ 100%]; **IR (νmax/cm^{-1})** 2965, 1643, 1492, 1247, 1154, 1049, 756, 548, 475; **HPLC** τ_R = 26.61 min (98.4% purity); Found: C, 77.26; H, 6.41; N, 7.48. Calc for $C_{24}H_{24}N_2O_2$: C, 77.39; H, 6.50; N, 7.52%

2-(9*H*-Carbazol-9-yl)-*N*-ethyl-*N*-(2- fluorobenzyl)acetamide (8d). White solid; yield 84% (183 mg, 0.508 mmol). **R_f** 0.56 (ethyl acetate/hexane, 3:7 v/v); **mp** 131–133 °C; **^{1}H NMR (300 MHz, $CDCl_3$) δ** = 8.10 – 8.01 (m, 2H, Ar**H**), 7.46 – 7.38 (m, 2H, Ar**H**) 7.32 – 7.18 (m, 5H, Ar**H**), 7.11 – 6.99 (m, 3H, Ar**H**),

5.07 (s, 2H, C**H**$_2$CO), 4.67 (s, 2H, C**H**$_2$Ph), 3.42 (q, *J* = 7.1 Hz, 2H, C**H**$_2$CH$_3$), 1.11 (t, *J* = 7.1 Hz, 3H, CH$_2$C**H**$_3$); **^{13}C NMR (75 MHz, CDCl$_3$) δ =** 167.21 (**C**O), 160.32 (d, *J* = 248.0 Hz, Ar), 140.72 (2×Ar), 130.92 (d, *J* = 3.6 Hz, Ar), 129.62 (d, *J* = 8.1 Hz, Ar), 125.92 (2×Ar), 125.86 (d, *J* = 7.8 Hz, Ar), 124.47 (d, *J* = 3.2 Hz, Ar), 123.23 (2×Ar), 120.46 (2×Ar), 120.33 (2×Ar), 115.42 (d, *J* = 21.8 Hz, Ar), 108.43 (2×Ar), 45.33 (**C**H$_2$CO), 44.76 (**C**H$_2$Ph), 41.63 (**C**H$_2$CH$_3$), 13.71 (CH$_2$**C**H$_3$); **^{19}F NMR (282 MHz, CDCl$_3$) δ =** –117.59 (Ar**F**); **LRMS (+ESI)** 383 [(M + Na)$^+$ 100%], 361 [(M + H)$^+$ 50%]; **IR (νmax/cm^{-1})** 3656, 2985, 2038, 1649, 1221, 744, 716, 420; Found: C, 76.58; H, 5.80; N, 7.76. Calc for $C_{23}H_{21}FN_2O$: C, 76.64; H, 5.87; N, 7.77%

2-(9*H*-Carbazol-9-yl)-*N*-ethyl-*N*-(3-fluorobenzyl)acetamide (8e). White solid; yield 92% (200 mg, 0.555 mmol). **R$_f$** 0.38 (ethyl acetate/hexane, 3:7 v/v); **mp** 135–137 °C; **^{1}H NMR (300 MHz, CDCl$_3$) δ** = 8.12 – 8.01 (m, 2H, Ar**H**), 7.53 – 7.33 (m, 2H, Ar**H**) 7.28 – 7.19 (m, 6H, Ar**H**), 6.98 – 6.94 (m, 2H, Ar**H**), 5.12 (s, 2H, C**H**$_2$CO), 4.57 (s, 2H, C**H**$_2$Ph), 3.35 (q, *J* = 7.1 Hz, 2H, C**H**$_2$CH$_3$), 1.11 (m, *J* = 7.1 Hz, 3H, CH$_2$C**H**$_3$); **^{13}C NMR (75 MHz, CDCl$_3$) δ =** 168.18 (**C**O), 161.70 (d, *J* = 252.1 Hz, Ar), 140.20 (2×Ar), 130.61 (d, *J* = 5.8 Hz, Ar), 126.56 (2×Ar), 125.98 (d, *J* = 8.3 Hz, Ar), 123.50 (2×Ar), 122.60 (d, *J* = 4.2 Hz, Ar), 120.71 (2×Ar), 120.50 (2×Ar), 119.78 (d, *J* = 20.8 Hz, Ar), 114.45 (d, *J* = 22.0 Hz, Ar), 108.53 (2×Ar), 47.12 (**C**H$_2$CO), 42.54 (**C**H$_2$Ph), 41.64 (**C**H$_2$CH$_3$), 13.65 (CH$_2$**C**H$_3$); **^{19}F NMR (282 MHz, CDCl$_3$) δ =** –114.84 (Ar**F**); **LRMS (+ESI)** 383 [(M + Na)$^+$ 100%], 361 [(M + H)$^+$ 50%]; **IR (νmax/cm^{-1})** 3671, 2987, 1654, 1454, 1393, 1230, 1066, 879, 445; Found: C, 75.77; H, 5.96; N, 7.89. Calc for $C_{23}H_{21}FN_2O$: C, 76.64; H, 5.87; N, 7.77%

2-(9*H*-Carbazol-9-yl)-*N*-ethyl-*N*-(4-fluorobenzyl)acetamide (8f). White solid; yield 87% (188 mg, 0.522 mmol). **R$_f$** 0.49 (ethyl acetate/hexane, 3:7 v/v); **mp** 165–167 °C; **^{1}H NMR (300 MHz, CDCl$_3$) δ** = 8.10 (dd, *J* = 24.9, 7.8 Hz, 2H, Ar**H**), 7.49 – 7.31 (m, 2H, Ar**H**), 7.28 – 7.19 (m, 6H, Ar**H**), 6.99 – 6.97 (m, 2H, Ar**H**), 5.11 (s, 2H, C**H**$_2$CO), 4.56 (s, 2H, C**H**$_2$Ph), 3.34 (t, *J* = 7.1 Hz, 2H, C**H**$_2$CH$_3$), 1.03 (t, *J* = 7.1 Hz, 3H, CH$_2$C**H**$_3$); **^{13}C NMR (75 MHz, CDCl$_3$) δ =** 166.69 (**C**O), 159.97 (d, *J* = 251.4 Hz, Ar), 140.58 (2×Ar), 133.68 (d, *J* = 3.3 Hz, Ar), 128.87 (d, *J* = 8.1 Hz, 2×Ar), 125.93 (2×Ar), 123.49 (2×Ar),

120.70 (2×Ar), 120.46 (2×Ar), 115.53 (d, J = 22.0 Hz, 2×Ar), 108.54 (2×Ar), 45.46 (**C**H_2CO), 42.16 (**C**H_2Ph), 41.26 (**C**$H_2$$CH_3$), 13.63 ($CH_2$**C**$H_3$); **^{19}F NMR (282 MHz, $CDCl_3$) δ =** –114.94 (Ar**F**); **LRMS (+ESI)** 383 [(M + Na)$^+$ 100%], 361 [(M + H)$^+$ 50%]; **IR (νmax/cm^{-1})** 3269, 2986, 1642, 1486, 1325, 1216, 1066, 745, 424; Found: C, 76.62; H, 5.75; N, 7.74. Calc for $C_{23}H_{21}FN_2O$: C, 76.64; H, 5.87; N, 7.77%

Methyl 2-(9*H*-carbazol-9-yl)acetate (9). Purification was achieved by recrystallisation in isopropanol. White solid; yield 81% (6.3 g, 26.3 mmol). **R_f** 0.57 (ethyl acetate/hexane, 1:4 v/v); **mp** 107–109 °C; **^{1}H NMR (300 MHz, $CDCl_3$) δ =** 8.07 (d, J = 7.7 Hz, 2H, Ar**H**), 7.50 – 7.39 (m, 2H, Ar**H**), 7.31 – 7.17 (m, 4H, Ar**H**), 4.93 (s, 2H, C**H$_2$**), 3.66 (s, 3H, C**H$_3$**); **^{13}C NMR (75 MHz, $CDCl_3$) δ =** 169.06 (**C**O), 140.54 (2×Ar), 126.02 (2×Ar), 123.27 (2×Ar), 120.51 (2×Ar), 119.74 (2×Ar), 108.36 (2×Ar), 52.52 (**C**H_3), 44.62 (**C**H_2); **LRMS (+ESI)** 262 [(M + Na)$^+$ 50%], 240 [(M + H)$^+$ 100%]; **IR (νmax/cm^{-1})** 3050, 1728, 1484, 1452, 1356, 1262, 1207, 998, 750, 718, 627**;** Found: C, 75.35; H, 5.38; N, 5.84 Calc for $C_{15}H_{13}NO_2$: C, 75.30; H, 5.48; N, 5.85%

2-(9*H*-carbazol-9-yl)acetic acid (10). Compound **9** (2.0 g, 8.36 mmol, 1.0 equiv.) and lithium hydroxide (800 mg, 33.4 mmol, 4.0 equiv.) were dissolved in a solution of tetrahydrofuran/water (20 mL, 1:1 v/v). The reaction mixture was stirred at reflux for 4 hours. The reaction mixture was then cooled to ambient temperature and the organic solvent evaporated to dryness. The remaining portion was diluted with ethyl acetate and acidified with aqueous hydrochloric (2 M, 10 mL), then extracted with ethyl acetate (3×10 mL). The combined organic extracts were dried over anhydrous magnesium sulfate and concentrated *in vacuo*. Purification by trituration in diethyl ether furnished the desired product as a colorless powder (1.36 g, 6.04 mmol, 72%). **R_f** 0.31 (methanol/dichloromethane, 1:9 v/v); **mp** 192 °C; **^{1}H NMR (300 MHz, DMSO) δ =** 8.12 (d, J = 7.7 Hz, 2H, Ar**H**), 7.58 – 7.35 (m, 4H, Ar**H**), 7.21 (t, J = 7.3 Hz, 2H, Ar**H**), 5.14 (s, 2H, C**H$_2$**), *OH proton not observed*; **^{13}C NMR (75 MHz, DMSO) δ =** 170.26 (**C**O), 140.27 (2×Ar), 125.84 (2×Ar), 122.14 (2×Ar), 120.11 (2×Ar), 119.24 (2×Ar), 108.98 (2×Ar), 43.82 (**C**H_2); **LRMS (-ESI)** 224 [(M + H)$^-$ 100%]; **IR (νmax/cm^{-1})** 3024, 1700, 1484, 1403, 1323, 1208, 1152,

920, 750, 720, 565, 419; Found: C, 74.59; H, 4.87; N, 6.21 Calc for $C_{14}H_{11}NO_2$: C, 74.65; H, 4.92; N, 6.22%

2-(9*H*-Carbazol-9-yl)-*N*-ethyl-*N*-(2-(trifluoromethyl)benzyl)acetamide (11a). White solid; yield 68% (124 mg, 0.302 mmol). $\mathbf{R_f}$ 0.44 (ethyl acetate/hexane, 3:7 v/v); **mp** 220–222 °C; **^{1}H NMR (300 MHz, $CDCl_3$) δ =** 8.11 (d, *J* = 7.7 Hz, 1H, Ar**H**), 8.00 (d, *J* = 7.7 Hz, 1H, Ar**H**), 7.65 (dd, *J* = 13.5, 7.7 Hz, 1H, Ar**H**), 7.54 – 7.10 (m, 9H, Ar**H**), 5.09 (s, 2H, C$\mathbf{H_2}$CO), 4.84 (s, 2H, C$\mathbf{H_2}$Ph), 3.36 (q, *J* = 7.1 Hz, 2H, C$\mathbf{H_2}$$CH_3$), 1.03 (t, *J* = 7.1 Hz, 3H, CH_2C$\mathbf{H_3}$); **^{13}C NMR (75 MHz, $CDCl_3$) δ =** 166.26 (**C**O), 140.65 (2×Ar), 132.18 (Ar), 131.04 (q, *J* = 3.2 Hz, Ar), 128.59 (q, *J* = 33.8 Hz Ar), 127.77 (q, *J* = 3.2 Hz, Ar), 127.20 (Ar), 126.01 (Ar), 125.82 (2×Ar), 124.42 (q, *J* = 271.2 Hz, **C**F_3), 123.31 (2×Ar), 120.55 (2×Ar), 119.62 (2×Ar), 108.44 (2×Ar), 47.74 (**C**H_2CO), 45.19 (**C**H_2Ph), 40.96 (**C**$H_2$$CH_3$), 13.58 ($CH_2$**C**$H_3$); **^{19}F NMR (282 MHz, $CDCl_3$) δ =** –60.77 (C**F**$_3$); **IR (vmax/cm^{-1})** 3052, 1653, 1463, 1320, 1260, 1113, 1064, 1014, 829, 740, 716, 596, 417; **LRMS (+ESI)** 433 [$(M + Na)^+$ 100%], 411 [$(M + H)^+$ 40%]; Found: C, 70.29; H, 5.11; N, 6.52. Calc for $C_{24}H_{21}F_3N_2O$: C, 70.23; H, 5.16; N, 6.83%

2-(9*H*-Carbazol-9-yl)-*N*-ethyl-*N*-(3-(trifluoromethyl)benzyl)acetamide (11b). White solid; yield 76% (138 mg, 0.336 mmol). $\mathbf{R_f}$ 0.44 (ethyl acetate/hexane, 3:7 v/v); **mp** 158–160 °C; **^{1}H NMR (300 MHz, $CDCl_3$) δ =** 8.10 (d, *J* = 7.7 Hz, 1H, Ar**H**), 7.92 (d, *J* = 7.7 Hz, 1H, Ar**H**), 7.66 – 7.01 (m, 9H), 6.84 (d, *J* = 7.9 Hz, 1H, Ar**H**), 5.06 (s, 2H, C$\mathbf{H_2}$CO), 4.60 (s, 2H, C$\mathbf{H_2}$Ph), 3.36 (q, *J* = 7.3 Hz, 2H, C$\mathbf{H_2}$$CH_3$), 1.03 (t, *J* = 7.3 Hz, 3H, CH_2C$\mathbf{H_3}$); **^{13}C NMR (75 MHz, $CDCl_3$) δ =** 167.48 (**C**O), 141.36 (Ar), 140.62 (2×Ar), 131.61 (Ar), 131.33 (q, *J* = 34.0 Hz, Ar), 128.33 (Ar), 125.99 (q, *J* = 3.4 Hz, Ar), 125.66 (2×Ar), 125.51 (q, *J* = 272.3 Hz**,** **C**F_3), 123.27 (2×Ar), 123.12 (q, *J* = 3.4 Hz, Ar), 120.55 (2×Ar), 119.62 (2×Ar), 108.37 (2×Ar), 48.39 (**C**H_2CO), 45.49 (**C**H_2Ph), 41.76 (**C**$H_2$$CH_3$), 13.67 ($CH_2$**C**$H_3$); **^{19}F NMR (282 MHz, $CDCl_3$) δ =** –62.53 (C**F**$_3$); **IR (vmax/cm^{-1})** 3053**,** 1653, 1464, 1321, 1260, 1321, 1160, 1113, 1064, 1014, 829, 740, 716, 596; **LRMS (+ESI)** 433 [$(M + Na)^+$ 100%], 411 [$(M + H)^+$ 40%]; Found: C, 70.19; H, 5.09; N, 6.62. Calc for $C_{24}H_{21}F_3N_2O$: C, 70.23; H, 5.16; N, 6.83%

2-(9*H*-Carbazol-9-yl)-*N*-ethyl-*N*-(4-(trifluoromethyl)benzyl)acetamide (11c). White solid; yield 81% (147 mg, 0.358 mmol). $\mathbf{R_f}$ 0.44 (ethyl acetate/hexane, 3:7 v/v); **mp** 171–173 °C; **^{1}H NMR (300 MHz, $CDCl_3$) δ =** 8.10 (d, *J* = 7.8 Hz, 1H, Ar**H**), 7.92 (d, *J* = 7.8 Hz, 1H, Ar**H**), 7.47 – 7.12 (m, 9H, Ar**H**), 6.84 (d, *J* = 7.8 Hz, 1H, Ar**H**), 5.10 (s, 2H, C$\mathbf{H_2}$CO), 4.63 (s, 2H, C$\mathbf{H_2}$Ph), 3.34 (q, *J* = 7.1 Hz, 2H, C$\mathbf{H_2}$$CH_3$), 1.02 (t, *J* = 7.1 Hz, 3H, CH_2C$\mathbf{H_3}$); **^{13}C NMR (75 MHz, $CDCl_3$) δ =** 167.41 (**C**O), 141.36 (Ar), 140.63 (2×Ar), 132.00 (q, *J* = 33.6 Hz, Ar), 128.32 (2×Ar), 126.02 (2×Ar), 125.98 (q, *J* = 3.4 Hz, 2×Ar), 125.52 (**C**F_3), 123.27 (2×Ar), 120.42 (2×Ar), 119.60 (2×Ar), 108.38 (2×Ar), 48.40 (**C**H_2CO), 46.41 (**C**H_2Ph), 41.75 (**C**H_2CH_3), 13.68 (CH_2**C**H_3); **^{19}F NMR (282 MHz, $CDCl_3$) δ =** –62.53 (C$\mathbf{F_3}$); **IR (vmax/cm^{-1})** 3043, 1654, 1455, 1326, 1260, 1162, 1123, 1065, 830, 740, 717, 597; **LRMS (+ESI)** 433 [(M + Na)$^+$ 100%], 411 [(M + H)$^+$ 40%]; Found: C, 70.22; H, 5.11; N, 6.52. Calc for $C_{24}H_{21}F_3N_2O$: C, 70.23; H, 5.16; N, 6.83%

2-(9*H*-Carbazol-9-yl)-*N*-ethyl-*N*-(pyridin-2-ylmethyl)acetamide (12a). White solid; yield 78% (119 mg, 0.347 mmol). $\mathbf{R_f}$ 0.71 (methanol/dichloromethane, 1:9 v/v); **mp** 195–197 °C; **^{1}H NMR (300 MHz, $CDCl_3$) δ =** 8.32 (d, *J* = 4.9 Hz, 1H, Ar**H**), 8.19 (s, 1H, Ar**H**), 8.04 (d, *J* = 7.6 Hz, 2H, Ar**H**), 7.49 – 7.44 (m, 2H, Ar**H**), 7.35 – 7.23 (m, 5H, Ar**H**), 7.11 – 7.06 (m, 1H, Ar**H**), 4.95 (s, 2H, C$\mathbf{H_2}$CO), 4.31 (s, 2H, C$\mathbf{H_2}$Ph), 3.43 (q, *J* = 7.1 Hz, 2H, C$\mathbf{H_2}$$CH_3$), 1.02 (t, *J* = 7.1 Hz, 3H, CH_2C$\mathbf{H_3}$); **^{13}C NMR (75 MHz, $CDCl_3$) δ** = 168.25 (**C**O), 155.92 (Ar), 148.96 (Ar), 140.40 (2×Ar), 136.55 (Ar), 126.33 (2×Ar), 123.52 (2×Ar), 122.19 (Ar), 121.39 (Ar), 120.59 (2×Ar), 120.22 (2×Ar), 108.68 (2×Ar), 47.19 (**C**H_2CO), 44.22 (**C**H_2Ph), 40.39 (**C**H_2CH_3), 13.36 (CH_2**C**H_3); **IR (vmax/cm^{-1})** 3286, 1650, 1590, 1485, 1324, 1209, 769, 745, 543; **LRMS (+ESI)** 366 [(M + Na)$^+$ 100%], 344 [(M + H)$^+$ 30%]; Found: C, 76.88; H, 6.14; N, 12.24 Calc for $C_{22}H_{21}N_3O$: C, 76.94; H, 6.16; N, 12.24%

2-(9*H*-Carbazol-9-yl)-*N*-ethyl-*N*-(pyridin-3-ylmethyl)acetamide (12b). White solid; yield 76% (116 mg, 0.338 mmol). $\mathbf{R_f}$ 0.63 (methanol/dichloromethane, 1:9 v/v); **mp** 228–230 °C; **^{1}H NMR (300 MHz, $CDCl_3$) δ =** 8.38 (d, *J* = 4.8 Hz, 1H, Ar**H**), 8.27 (s, 1H, Ar**H**), 8.08 (d, *J* = 7.7 Hz, 2H, Ar**H**), 7.50 – 7.44 (m, 2H, Ar**H**), 7.39 – 7.25 (m, 5H, Ar**H**), 7.15 – 7.10 (m, 1H, Ar**H**), 4.98 (s, 2H, C$\mathbf{H_2}$CO), 4.35 (s, 2H,

C**H**$_2$Pyr), 3.41 (q, *J* = 7.1 Hz, 2H, C**H**$_2$CH$_3$), 1.02 (t, *J* = 7.1 Hz, 3H, CH$_2$C**H**$_3$); **^{13}C NMR (75 MHz, CDCl$_3$) δ =** 168.15 (**C**O), 148.73 (Ar), 143.14 (Ar), 140.21 (2×Ar), 135.07 (Ar), 133.23 (Ar), 126.54 (2×Ar), 123.46 (Ar), 123.41 (2×Ar), 120.67 (2×Ar), 120.45 (2×Ar), 108.48 (2×Ar), 47.03 (**C**H$_2$CO), 41.38 (**C**H$_2$Ph), 40.69 (**C**H$_2$CH$_3$), 13.29 (CH$_2$**C**H$_3$); **IR (vmax/cm^{-1})** 3281, 1662, 1461, 1324, 1255, 1119, 1066, 746, 719; **LRMS (+ESI)** 366 [(M + Na)$^+$ 100%], 344 [(M + H)$^+$ 40%]; Found: C, 76.84; H, 6.04; N, 12.22 Calc for $C_{22}H_{21}N_3O$: C, 76.94; H, 6.16; N, 12.24%

2-(9*H*-Carbazol-9-yl)-*N*-ethyl-*N*-(pyridin-4-ylmethyl)acetamide (12c). White solid; yield 84% (128 mg, 0.373 mmol). **R$_f$** 0.63 (methanol/dichloromethane, 1:9 v/v); **mp** 203–205 °C; **^{1}H NMR (300 MHz, CDCl$_3$) δ =** 8.35 (d, *J* = 4.9 Hz, 1H, Ar**H**), 8.22 (s, 1H, Ar**H**), 8.06 (d, *J* = 7.7 Hz, 2H, Ar**H**), 7.51 – 7.45 (m, 2H, Ar**H**), 7.36 – 7.25 (m, 5H, Ar**H**), 7.12 – 7.08 (m, 1H, Ar**H**), 4.97 (s, 2H, C**H**$_2$CO), 4.33 (s, 2H, C**H**$_2$Pyr), 3.42 (q, *J* = 7.1 Hz, 2H, C**H**$_2$CH$_3$), 1.03 (t, *J* = 7.1 Hz, 3H, CH$_2$C**H**$_3$); **^{13}C NMR (75 MHz, CDCl$_3$) δ =** 168.32 (**C**O), 148.76 (2×Ar), 148.62 (Ar), 140.18 (2×Ar), 126.55 (2×Ar), 123.48 (2×Ar), 123.35 (2×Ar), 120.69 (2×Ar), 120.49 (2×Ar), 108.45 (2×Ar), 47.09 (**C**H$_2$CO), 40.66 (**C**H$_2$Ph), 40.21 (**C**H$_2$CH$_3$), 13.28 (CH$_2$**C**H$_3$); **IR (vmax/cm^{-1})** 3052, 1653, 1463, 1321, 1260, 1160, 1113, 1064, 1014, 829, 716, 596; **LRMS (+ESI)** 366 [(M + Na)$^+$ 100%], 344 [(M + H)$^+$ 40%]; Found: C, 76.56; H, 6.11; N, 12.24 Calc for $C_{22}H_{21}N_3O$: C, 76.94; H, 6.16; N, 12.24%

2-(9*H*-Carbazol-9-yl)-*N*-ethyl-*N*-(2-nitrobenzyl)acetamide (13a). White solid; yield 91% (157 mg, 0.405 mmol). **R$_f$** 0.28 (ethyl acetate/hexane, 3:7 v/v); **mp** 225–227 °C; **^{1}H NMR (300 MHz, CDCl$_3$) δ** = 8.09 (d, *J* = 8.0 Hz, 2H, Ar**H**), 7.80 (d, *J* = 8.0 Hz, 1H, Ar**H**), 7.52 – 6.89 (m, 8H, Ar**H**), 6.58 (d, *J* = 7.8 Hz, 1H, Ar**H**), 5.12 (s, 2H, C**H**$_2$CO), 4.91 (s, 2H, C**H**$_2$Ph), 3.39 (q, *J* = 7.1 Hz, 2H, C**H**$_2$CH$_3$), 1.11 (t, *J* = 7.1 Hz, 3H, CH$_2$C**H**$_3$); **^{13}C NMR (75 MHz, CDCl$_3$) δ =** 168.64 (**C**O), 145.95 (Ar), 139.91 (2×Ar), 133.46 (Ar), 127.66 (Ar), 126.45 (Ar), 126.01 (2×Ar), 125.29 (Ar), 123.30 (2×Ar), 122.88 (Ar), 120.09 (2×Ar), 119.53 (2×Ar), 108.48 (2×Ar), 49.29 (**C**H$_2$CO), 47.02 (**C**H$_2$Ph), 42.65 (**C**H$_2$CH$_3$), 13.84 (CH$_2$**C**H$_3$); **LRMS (+ESI)** 410 [(M + Na)$^+$ 100%], 388 [(M + H)$^+$ 40%]; **IR (vmax/cm^{-1})** 3091, 1659, 1541, 1460,

1324, 1254, 1209, 1152, 934, 746, 717, 602, 547, 421; Found: C, 71.35; H, 5.38; N, 10.81 Calc for $C_{23}H_{21}N_3O_3$: C, 71.30; H, 5.46; N, 10.85%

2-(9*H*-Carbazol-9-yl)-*N*-ethyl-*N*-(3-nitrobenzyl)acetamide (13b). White solid; yield 86% (148 mg, 0.382 mmol). $\mathbf{R_f}$ 0.28 (ethyl acetate/hexane, 3:7 v/v); **mp** 133–135 °C; **^{1}H NMR (300 MHz, $CDCl_3$) δ** = 8.12 (d, *J* = 7.8 Hz, 2H, Ar**H**), 8.04 (d, *J* = 6.5 Hz, 1H, Ar**H**), 7.91 (s, 1H, Ar**H**), 7.56 – 7.48 (m, 2H, Ar**H**), 7.42 – 7.29 (m, 6H, Ar**H**), 5.12 (s, 2H, C$\mathbf{H_2}$CO), 4.65 (s, 2H, C$\mathbf{H_2}$Ph), 3.42 (q, *J* = 7.1 Hz, 2H, C$\mathbf{H_2}$$CH_3$), 1.06 (t, *J* = 7.1 Hz, 3H, CH_2C$\mathbf{H_3}$); **^{13}C NMR (75 MHz, $CDCl_3$) δ =** 167.42 (**C**O), 148.32 (Ar), 142.88 (Ar), 140.63 (2×Ar), 135.40 (Ar), 129.96 (Ar), 125.23 (2×Ar), 124.36 (Ar), 123.25 (2×Ar), 122.50 (Ar), 120.22 (2×Ar), 119.63 (2×Ar), 108.34 (2×Ar), 48.39 (**C**H_2CO), 45.31 (**C**H_2Ph), 42.14 (**C**H_2CH_3), 13.81 (CH_2**C**H_3); **IR (νmax/cm^{-1})** 3091, 1659, 1541, 1460, 1324, 1254, 1209, 1152, 934, 746, 717, 602, 547, 421; **LRMS (+ESI)** 410 [(M + Na)$^+$ 100%], 388 [(M + H)$^+$ 40%]; Found: C, 71.28; H, 5.42; N, 10.83 Calc for $C_{23}H_{21}N_3O_3$: C, 71.30; H, 5.46; N, 10.85%

2-(9*H*-Carbazol-9-yl)-*N*-ethyl-*N*-(4-nitrobenzyl)acetamide (13c). White solid; yield 87% (150 mg, 0.388 mmol). $\mathbf{R_f}$ 0.28 (ethyl acetate/hexane, 3:7 v/v); **mp** 239–241 °C; **^{1}H NMR (300 MHz, $CDCl_3$) δ =** 8.12 – 8.05 (m, 3H, Ar**H**), 7.80 (d, *J* = 8.0 Hz, 1H, Ar**H**), 7.53 – 7.14 (m, 8H, Ar**H**), 5.07 (s, 2H, C$\mathbf{H_2}$CO), 4.58 (s, 2H, C$\mathbf{H_2}$Ph), 3.40 (q, *J* = 7.1 Hz, 2H, C$\mathbf{H_2}$$CH_3$), 1.01 (t, *J* = 7.1 Hz, 3H, CH_2C$\mathbf{H_3}$); **^{13}C NMR (75 MHz, $CDCl_3$) δ =** 168.24 (**C**O), 148.39 (Ar), 146.79 (Ar), 140.77 (2×Ar), 129.73 (2×Ar), 126.03 (2×Ar), 123.75 (2×Ar), 122.98 (2×Ar), 120.59 (2×Ar), 119.73 (2×Ar), 108.08 (2×Ar), 46.19 (**C**H_2CO), 44.46 (**C**H_2Ph), 40.62 (**C**H_2CH_3), 13.30 (CH_2**C**H_3); **IR (νmax/cm^{-1})** 3086, 1660, 1533, 1460, 1344, 1255, 1120, 848, 752, 723, 587, 426; **LRMS (+ESI)** 410 [(M + Na)$^+$ 100%], 388 [(M + H)$^+$ 40%]; Found: C, 71.28; H, 5.41; N, 10.84 Calc for $C_{23}H_{21}N_3O_3$: C, 71.30; H, 5.46; N, 10.85%

2-(9*H*-Carbazol-9-yl)-*N*,*N*-dimethylacetamide (14a). White solid; yield 83% (93 mg, 0.369 mmol). $\mathbf{R_f}$ 0.13 (ethyl acetate/hexane, 3:7 v/v); **mp** 126–128 °C; **^{1}H NMR (400 MHz, $CDCl_3$) δ =** 8.08 (d, *J* = 7.7 Hz, 2H, Ar**H**), 7.55 – 7.16 (m, 6H, Ar**H**), 5.06 (s, 2H, C$\mathbf{H_2}$CO), 3.04 (s, 6H, 2×C$\mathbf{H_3}$); **^{13}C NMR (101 MHz, $CDCl_3$) δ =** 167.27 (**C**O), 140.67 (2×Ar), 125.95 (2×Ar), 123.21 (2×Ar), 120.45 (2×Ar), 119.48

(2×Ar), 108.50 (2×Ar), 45.59 (**C**H_2CO), 36.71 (**C**H_3), 36.12 (**C**H_3); **IR (vmax/cm^{-1})** 2969, 1650, 1598, 1461, 1329, 1257, 1214, 1153, 1048, 744, 725, 693, 556, 421; **LRMS (+ESI)** 275 [(M + Na)$^+$ 100%], 253 [(M + H)$^+$ 50%]; Found: C, 76.18; H, 6.29; N, 11.21 Calc for $C_{16}H_{16}N_2O$: C, 76.16; H, 6.39; N, 11.10%

***N*-(2-Acetamidobenzyl)-2-(9*H*-carbazol-9-yl)-*N*-ethylacetamide (15a).** White solid; yield 70% (72 mg, 0.180 mmol). **R_f** 0.69 (methanol/dichloromethane, 1:9 v/v); **mp** 210–212 °C; **^{1}H NMR (300 MHz, $CDCl_3$) δ** = 9.11 (s, 1H, N**H**), 8.11 (d, *J* = 7.8 Hz, 2H, Ar**H**), 7.51 – 7.09 (m, 9H, Ar**H**), 7.03 (t, *J* = 7.4 Hz, 1H, Ar**H**), 5.08 (s, 2H, C**H$_2$**CO), 4.56 (s, 2H, C**H$_2$**Ph), 3.45 (q, *J* = 7.1 Hz, 2H, C**H$_2$**CH_3), 1.63 (s, 3H, AcC**H$_3$**), 1.19 (t, *J* = 7.1 Hz, 3H, CH_2C**H$_3$**); **^{13}C NMR (75 MHz, $CDCl_3$) δ** = 169.83 (**C**O), 168.26 (**C**O), 140.79 (2×Ar), 137.94 (Ar), 131.50 (Ar), 129.71 (Ar), 126.03 (2×Ar), 123.90 (Ar), 123.22 (2×Ar), 123.01 (Ar), 121.20 (Ar), 120.59 (2×Ar), 119.73 (2×Ar), 108.08 (2×Ar), 46.22 (**C**H_2Ph), 44.53 (**C**H_2CO), 40.67 (**C**H_2CH_3), 24.18 (Ac**C**H_3), 13.28 (CH_2**C**H_3); **LRMS (+ESI)** 422 [(M + Na)$^+$ 100%], 400 [(M + H)$^+$ 35%]; **IR (vmax/cm^{-1})** 3319, 3050, 1635, 1544, 1452, 1295, 1265, 1214, 745, 721, 422; Found: C, 75.10; H, 6.28; N, 10.49 Calc for $C_{25}H_{25}N_3O_2$: C, 75.16; H, 6.31; N, 10.52%

***N*-(3-Acetamidobenzyl)-2-(9*H*-carbazol-9-yl)-*N*-ethylacetamide (15b).** White solid; yield 77% (79 mg, 0.198 mmol). **R_f** 0.67 (methanol/dichloromethane, 1:9 v/v); **mp** 179–181 °C; **^{1}H NMR (300 MHz, $CDCl_3$) δ** = 9.16 (s, 1H, N**H**), 8.11 (d, *J* = 7.7 Hz, 2H, Ar**H**), 7.52 – 6.94 (m, 10H, Ar**H**), 5.17 (s, 2H, C**H$_2$**CO), 4.68 (s, 2H, C**H$_2$**Ph), 3.42 (q, *J* = 7.1 Hz, 2H, C**H$_2$**CH_3), 2.06 (s, 3H, AcC**H$_3$**), 1.06 (t, *J* = 7.1 Hz, 3H, CH_2C**H$_3$**); **^{13}C NMR (75 MHz, $CDCl_3$) δ** = 169.69 (**C**O), 168.19 (**C**O), 140.62 (2×Ar), 138.94 (Ar), 136.11 (Ar), 128.24 (Ar), 126.03 (2×Ar), 123.31 (2×Ar), 122.89 (Ar), 121.13 (Ar), 120.49 (2×Ar), 119.96 (Ar), 119.69 (2×Ar), 108.39 (2×Ar), 46.33 (**C**H_2CO), 44.72 (**C**H_2Ph), 40.55 (**C**H_2CH_3), 24.19 (Ac**C**H_3), 13.26 (CH_2**C**H_3); **IR (vmax/cm^{-1})** 3291, 2936, 1640, 1539, 1442, 1345, 1213, 746, 725, 422; **LRMS (+ESI)** 422 [(M + Na)$^+$ 100%], 400 [(M + H)$^+$ 35%]; Found: C, 75.11; H, 6.28; N, 10.53 Calc for $C_{25}H_{25}N_3O_2$: C, 75.16; H, 6.31; N, 10.52%

***N*-(4-Acetamidobenzyl)-2-(9*H*-carbazol-9-yl)-*N*-ethylacetamide (15c).** White solid; yield 73% (75 mg, 0.188 mmol). **R_f** 0.67 (methanol/dichloromethane, 1:9 v/v); **mp** 172–174 °C; **^{1}H NMR (300 MHz,**

$CDCl_3$) δ = 9.14 (s, 1H, N**H**), 8.09 (d, *J* = 7.7 Hz, 2H, Ar**H**), 7.52 – 6.94 (m, 10H, Ar**H**), 5.06 (s, 2H, C$\mathbf{H_2}$CO), 4.56 (s, 2H, C$\mathbf{H_2}$Ph), 3.38 (q, *J* = 7.1 Hz, 2H, C$\mathbf{H_2}CH_3$), 2.03 (s, 3H, AcC$\mathbf{H_3}$), 1.09 (t, *J* = 7.1 Hz, 3H, $CH_2C\mathbf{H_3}$); **^{13}C NMR (75 MHz, $CDCl_3$) δ =** 169.80 (**C**O), 168.24 (**C**O), 139.79 (2×Ar), 137.94 (Ar), 131.55 (Ar), 129.73 (2×Ar), 126.03 (2×Ar), 123.31 (2×Ar), 121.13 (2×Ar), 120.49 (2×Ar), 119.70 (2×Ar), 108.18 (2×Ar), 48.80 (**C**H_2CO), 44.51 (**C**H_2Ph), 41.56 (**C**H_2CH_3), 24.16 (Ac**C**H_3), 13.16 ($CH_2\mathbf{C}H_3$); **IR (νmax/cm^{-1})** 3282, 2925, 1643, 1529, 1410, 1367, 1213, 748, 721, 505, 422; **LRMS (+ESI)** 422 [(M + Na)$^+$ 100%], 400 [(M + H)$^+$ 40%]; Found: C, 75.09; H, 6.26; N, 10.55 Calc for $C_{25}H_{25}N_3O_2$: C, 75.16; H, 6.31; N, 10.52%

2-(3-Bromo-9*H*-carbazol-9-yl)-*N*-(3-methoxybenzyl)acetamide (17). Purification was achieved by recrystallisation in isopropanol. White solid; yield 93% (3.20 g, 7.56 mmol). **R_f** 0.19 (ethyl acetate/hexane, 3:7 v/v); **mp** 223–225 °C; **^{1}H NMR (400 MHz, DMSO) δ =** 8.77 (br s, 1H, N**H**), 8.41 (s, 1H, Ar**H**), 8.22 (d, *J* = 7.8 Hz, 1H, Ar**H**), 7.68 – 7.44 (m, 4H, Ar**H**), 7.26 – 7.23 (m, 2H, Ar**H**), 6.86 – 6.79 (m, 3H, Ar**H**), 5.12 (s, 2H, C$\mathbf{H_2}$CO), 4.29 (d *J* = 5.9 Hz, 2H, C$\mathbf{H_2}$Ph), 3.71 (s, 3H, OC$\mathbf{H_3}$); **^{13}C NMR (101 MHz, DMSO) δ =** 167.72 (**C**O), 159.79 (Ar), 141.45 (Ar), 141.12 (Ar), 139.93 (Ar), 129.80 (Ar), 128.43 (Ar), 126.95 (Ar), 124.74 (Ar), 123.22 (Ar), 121.80 (Ar), 121.22 (Ar), 119.94 (Ar), 119.84 (Ar), 113.09 (Ar), 112.91 (Ar), 111.92 (Ar), 111.62 (Ar), 110.06 (Ar), 55.42 (O**C**H_3), 46.13 (**C**H_2CO), 42.68 (**C**H_2Ph); **LRMS (+ESI)** 447/445 [(M + Na)$^+$ 100%], 425/423 [(M + H)$^+$ 10%]; **IR (νmax/cm^{-1})** 3269, 2979, 1648, 1597, 1546, 1489, 1457, 1438, 1380, 1264, 1246, 1210, 1078, 996, 690, 606, 412; Found: C, 62.29; H, 4.49; N, 6.58 Calc for $C_{22}H_{19}BrN_2O_2$: C, 62.42; H, 4.52; N, 6.62%

2-(3-Bromo-9*H*-carbazol-9-yl)-*N*-ethyl-*N*-(3-methoxybenzyl)acetamide (18a). White solid; yield 91% (970 mg, 2.15 mmol). **mp** 97–99 °C; **^{1}H NMR (400 MHz, $CDCl_3$) δ =** 8.27 (s, 1H, Ar**H**), 8.02 (d, *J* = 7.8 Hz, 1H, Ar**H**), 7.62 – 7.37 (m, 2H, Ar**H**), 7.37 – 7.12 (m, 3H, Ar**H**), 7.06 (d, *J* = 8.7 Hz, 1H, Ar**H**), 6.95 – 6.62 (m, 3H, Ar**H**), 4.95 (s, 2H, C$\mathbf{H_2}$CO), 4.60 (s, 2H, C$\mathbf{H_2}$Ph), 3.81 (s, 3H, OC$\mathbf{H_3}$), 3.46 (q, *J* = 7.1 Hz, 2H, C$\mathbf{H_2}CH_3$), 1.16 (t, *J* = 7.1 Hz, 3H, $CH_2C\mathbf{H_3}$); **^{13}C NMR (101 MHz, $CDCl_3$) δ =** 166.59 (**C**O), 159.92 (Ar), 141.06 (Ar), 139.47 (Ar), 130.25 (Ar), 129.62 (Ar), 128.55 (Ar), 126.68 (Ar), 126.54 (Ar),

124.99 (Ar), 123.22 (Ar), 120.54 (Ar), 119.92 (Ar), 119.77 (Ar), 117.94 (Ar), 113.22 (Ar), 111.63 (Ar), 110.03 (Ar), 108.73 (Ar), 55.24 (O**C**H_3), 50.12 (**C**H_2CO), 45.46 (**C**H_2Ph), 41.14 (**C**H_2CH_3), 12.78 (CH_2**C**H_3); **LRMS (+ESI)** 475/473 [$(M + Na)^+$ 100%], 453/451 [$(M + H)^+$ 50%]; **IR (vmax/cm^{-1})** 2970, 1651, 1598, 1461, 1329, 1258, 1213, 1048, 744, 693, 556, 421; Found: C, 64.02; H, 5.21; N, 6.16 Calc for $C_{24}H_{23}BrN_2O_2$: C, 63.87; H, 5.14; N, 6.21%

***N*-Ethyl-*N*-(3-methoxybenzyl)-2-(3-phenyl-9*H*-carbazol-9-yl)acetamide (18b)**

White solid; yield 72% (72 mg, 0.161 mmol). $\mathbf{R_f}$ 0.29 (ethyl acetate/hexane, 3:7 v/v); **mp** 68–70 °C; **^{1}H NMR (400 MHz, $CDCl_3$) δ =** 8.26 (s, 1H, Ar**H**), 8.16 (d, *J* = 7.8 Hz, 1H, Ar**H**), 7.81 – 7.72 (m, 2H, Ar**H**), 7.52 – 7.21 (m, 9H, Ar**H**), 6.89 – 6.75 (m, 2H, Ar**H**), 6.68 (s, 1H, Ar**H**), 5.09 (s, 2H, C$\mathbf{H_2}$CO), 4.63 (s, 2H, C$\mathbf{H_2}$Ph), 3.77 (s, 3H, OC$\mathbf{H_3}$), 3.52 (q, *J* = 7.1 Hz, 2H, C$\mathbf{H_2}CH_3$), 1.17 (t, *J* = 7.1 Hz, 3H, CH_2C$\mathbf{H_3}$); **^{13}C NMR (75 MHz, $CDCl_3$) δ =** 167.36 (**C**O), 160.33 (Ar), 141.21 (Ar), 140.70 (Ar), 139.70 (Ar), 138.88 (Ar), 134.11 (Ar), 129.60 (Ar), 128.84 (2×Ar), 127.32 (2×Ar), 126.80 (Ar), 126.72 (Ar), 126.06 (Ar), 124.02 (Ar) 123.62 (Ar), 120.78 (Ar), 120.57 (Ar), 119.36 (Ar), 119.23 (Ar), 113.13 (Ar), 111.57 (Ar), 108.74 (Ar), 108.59 (Ar), 55.19 (O**C**H_3), 48.38 (**C**H_2CO), 45.39 (**C**H_2Ph), 41.15 (**C**H_2CH_3), 13.69 (CH_2**C**H_3); **IR (vmax /cm^{-1})** 2975, 1642, 1450, 1362, 1214, 1078, 724, 697; **MS (+ESI):** m/z 471 [$(M + Na)^+$ 100%]; (Found (+ESI): $[M + Na]^+$, 471.1905. $C_{30}H_{28}N_2O_2Na^+$ requires 471.1900); **HPLC** τ_R =16.29 min (97.1% purity).

***N*-Ethyl-*N*-(3-methoxybenzyl)-2-(3-(4-methoxyphenyl)-9*H*-carbazol-9-yl)acetamide (18c).** White solid; yield 75% (79 mg, 0.165 mmol). $\mathbf{R_f}$ 0.23 (ethyl acetate/hexane, 3:7 v/v); **mp** 61–63 °C; **^{1}H NMR (400 MHz, $CDCl_3$) δ =** 8.33 (s, 1H, Ar**H**), 8.13 (d, *J* = 7.7 Hz, 1H, Ar**H**), 7.68 – 7.60 (m, 3H, Ar**H**), 7.55 – 7.19 (m, 4H, Ar**H**), 7.04 (d, *J* = 8.8, 2H, Ar**H**), 6.97 – 6.72 (m, 3H, Ar**H**), 6.68 (s, 1H, Ar**H**), 5.15 (s, 2H, C$\mathbf{H_2}$CO), 4.63 (s, 2H, C$\mathbf{H_2}$Ph), 3.90 (s, 3H, OC$\mathbf{H_3}$), 3.73 (s, 3H, OC$\mathbf{H_3}$), 3.48 (q, *J* = 7.0 Hz, 2H, C$\mathbf{H_2}CH_3$), 1.16 (t, *J* = 7.0 Hz, 3H, CH_2C$\mathbf{H_3}$); **^{13}C NMR (101 MHz, $CDCl_3$) δ =** 167.04 (**C**O), 159.98 (Ar), 158.60 (Ar), 141.20 (Ar), 139.96 (Ar), 138.85 (Ar), 137.97 (Ar), 134.78 (Ar), 129.58 (Ar), 128.28 (2×Ar), 126.08 (Ar), 125.96 (Ar), 125.28 (Ar), 123.37 (Ar), 120.56 (Ar), 119.57 (Ar), 119.44 (Ar), 118.49

(Ar), 118.07 (Ar), 114.21 (2×Ar), 113.12 (Ar), 108.70 (Ar), 108.55 (Ar), 55.40 (O**C**H_3), 55.20 (O**C**H_3), 48.37 (**C**H_2CO), 45.74 (**C**H_2Ph), 41.16 (**C**H_2CH_3), 12.77 (CH_2**C**H_3); **IR (νmax/cm^{-1})** 2970, 1651, 1598, 1461, 1329, 1258, 1213, 1048, 744, 725, 693, 556, 421; **LRMS (+ESI)** 501 [(M + Na)$^+$ 100%], 479 [(M + H)$^+$ 25%]; Found: C, 77.76; H, 6.33; N, 5.92 Calc for $C_{31}H_{30}N_2O_3$: C, 77.80; H, 6.32; N, 5.85%

2-(3-Bromo-9*H*-carbazol-9-yl)-*N*-(3-methoxybenzyl)-N-methylacetamide (19a). White solid; yield 93% (960 mg, 2.20 mmol). **R$_f$** 0.26 (ethyl acetate/hexane, 3:7 v/v); **mp** 67–69 °C; **^{1}H NMR (400 MHz, CDCl$_3$) δ =** 8.21 (s, 1H, Ar**H**), 8.02 (d, *J* = 7.8 Hz, 1H, Ar**H**), 7.54 – 7.47 (m, 2H, Ar**H**), 7.44 – 7.05 (m, 4H, Ar**H**), 6.83 – 6.67 (m, 3H, Ar**H**), 5.03 (s, 2H, C**H$_2$**CO), 4.60 (s, 2H, C**H$_2$**Ph), 3.82 (s, 3H, OC**H$_3$**), 2.94 (s, 3H, C**H$_3$**); **^{13}C NMR (101 MHz, CDCl$_3$) δ =** 167.39 (**C**O), 159.96 (Ar), 141.00 (Ar), 138.19 (Ar), 137.44 (Ar), 129.70 (Ar), 128.53 (Ar), 128.43 (Ar), 126.59 (Ar), 125.31 (Ar), 123.08 (Ar), 122.17 (Ar), 120.54 (Ar), 119.93 (Ar), 117.94 (Ar), 113.32 (Ar), 111.67 (Ar), 110.09 (Ar), 108.69 (Ar), 55.21 (O**C**H_3), 51.57 (**C**H_2CO), 45.42 (**C**H_2Ph), 34.23 (**C**H_3); **IR (νmax/cm^{-1})** 2933, 1651, 1597, 1475, 1330, 1258, 1146, 1051, 792, 743, 563, 421; **LRMS (+ESI)** 461/459 [(M + Na)$^+$ 100%]; Found: C, 63.13; H, 4.81; N, 6.45 Calc for $C_{23}H_{21}BrN_2O_2$: C, 63.17; H, 4.84; N, 6.41%

***N*-(3-Methoxybenzyl)-*N*-methyl-2-(3-phenyl-9*H*-carbazol-9-yl)acetamide (19b).** White solid; yield 73% (73 mg, 0.168 mmol). **R$_f$** 0.26 (ethyl acetate/hexane, 3:7 v/v); **mp** 121–123 °C; **^{1}H NMR (400 MHz, CDCl$_3$) δ =** 8.31 (s, 1H, Ar**H**), 8.15 (d, *J* = 7.8 Hz, 1H, Ar**H**), 7.80 – 7.64 (m, 3H, Ar**H**), 7.59 – 7.29 (m, 7H, Ar**H**), 7.19 – 7.00 (m, 1H, Ar**H**), 6.78 – 6.44 (m, 3H, Ar**H**), 5.02 (s, 2H, C**H$_2$**CO), 4.38 (s, 2H, C**H$_2$**Ph), 3.63 (s, 3H, OC**H$_3$**), 2.97 (s, 3H, C**H$_3$**); **^{13}C NMR (75 MHz, CDCl$_3$) δ =** 167.38 (**C**O), 159.79 (Ar), 141.62 (Ar), 140.69 (Ar), 139.70 (Ar), 138.87 (Ar), 134.11 (Ar), 129.64 (Ar), 128.89 (2×Ar), 127.34 (2×Ar), 126.79 (Ar), 126.73 (Ar), 126.09 (Ar), 124.06 (Ar), 123.66 (Ar), 120.81 (Ar) 120.51 (Ar), 119.38 (Ar), 119.23 (Ar), 113.34 (Ar), 112.26 (Ar), 108.75 (Ar), 108.61 (Ar), 55.09 (O**C**H_3), 47.27 (**C**H_2CO), 45.13 (**C**H_2Ph), 34.24 (**C**H_3); **LRMS (+ESI)** 457 [(M + Na)$^+$ 100%], 435 [(M + H)$^+$ 25%]; **IR (νmax/cm^{-1})** 3050, 2967, 1651, 1594, 1562, 1457, 1366, 1290, 1216, 1154, 1097, 1075, 1046, 996, 945, 811, 691, 595, 421; Found: C, 80.21; H, 6.05; N, 6.43 Calc for $C_{29}H_{26}N_2O_2$: C, 80.16; H, 6.03; N, 6.45%

***N*-(3-Methoxybenzyl)-2-(3-(4-methoxyphenyl)-9*H*-carbazol-9-yl)-*N*-methylacetamide (19c).** White solid; yield 77% (82 mg, 0.177 mmol). $\mathbf{R_f}$ 0.15 (ethyl acetate/hexane, 3:7 v/v); **mp** 62–64 °C; **^{1}H NMR (400 MHz, $CDCl_3$) δ =** 8.33 (s, 1H, Ar**H**), 8.17 (d, *J* = 7.8 Hz, 1H, Ar**H**), 7.77 – 7.71 (m, 3H, Ar**H**), 7.54 – 7.33 (m, 6H, Ar**H**), 7.14 – 7.10 (m, 1H, Ar**H**), 6.74 – 6.55 (m, 3H, Ar**H**), 5.05 (s, 2H, C$\mathbf{H_2}$CO), 4.41 (s, 2H, C$\mathbf{H_2}$Ph), 3.66 (s, 3H, OC$\mathbf{H_3}$), 3.62 (s, 3H, OC$\mathbf{H_3}$), 2.97 (s, 3H, C$\mathbf{H_3}$); **^{13}C NMR (101 MHz, $CDCl_3$) δ =** 167.97 (**C**O), 159.80 (Ar), 158.58 (Ar), 141.62 (Ar), 140.70 (Ar), 139.70 (Ar), 138.87 (Ar), 134.11 (Ar), 129.61 (Ar), 128.84 (2×Ar), 127.32 (Ar), 126.80 (Ar), 126.06 (Ar), 124.02 (Ar), 123.62 (Ar), 120.78 (Ar), 120.57 (Ar), 119.36 (Ar), 119.23 (Ar), 113.31 (2×Ar), 112.22 (Ar), 108.81 (Ar), 108.69 (Ar), 55.21 (O**C**H_3), 55.09 (O**C**H_3), 47.27 (**C**H_2CO), 43.13 (**C**H_2Ph), 34.33 (**C**H_3); **IR (νmax/cm^{-1})** 2969, 1652, 1599, 1462, 1330, 1258, 1214, 1152, 1048, 744, 725, 693, 556, 507, 422; **LRMS (+ESI)** 487 [(M + Na)$^+$ 100%], 465 [(M + H)$^+$ 50%]; Found: C, 77.58; H, 6.09; N, 5.99 Calc for $C_{30}H_{28}N_2O_3$: C, 77.56; H, 6.08; N, 6.03%

2-(3-(2-Chlorophenyl)-9*H*-carbazol-9-yl)-*N*-(3-methoxybenzyl)-*N*-methylacetamide (20a). White solid; yield 77% (58 mg, 0.124 mmol). $\mathbf{R_f}$ 0.43 (ethyl acetate/hexane, 3:7 v/v); **^{1}H NMR (400 MHz, $CDCl_3$) δ =** 8.16 (s, 1H, Ar**H**), 8.07 (d, *J* = 7.7 Hz, 1H, Ar**H**), 7.64 – 7.18 (m, 10H, Ar**H**), 7.70 – 6.62 (m, 3H, Ar**H**), 5.15 (s, 2H, C$\mathbf{H_2}$CO), 4.63 (s, 2H, C$\mathbf{H_2}$Ph), 3.74 (s, 3H, OC$\mathbf{H_3}$), 3.00 (s, 3H, C$\mathbf{H_3}$); **^{13}C NMR (101 MHz, $CDCl_3$) δ =** 167.26 (**C**O), 159.97 (Ar), 141.11 (Ar), 140.13 (Ar), 137.52 (Ar), 132.89 (Ar), 131.93 (Ar), 130.95 (Ar), 130.28 (Ar), 129.91 (Ar), 129.66 (Ar), 128.07 (Ar), 127.59 (Ar), 127.50 (Ar), 126.78 (Ar), 126.14 (Ar), 123.30 (Ar), 123.08 (Ar), 121.51 (Ar), 120.57 (Ar), 119.72 (Ar), 118.04 (Ar), 113.43 (Ar), 111.59 (Ar), 108.63 (Ar), 55.21 (O**C**H_3), 51.60 (**C**H_2CO), 45.66 (**C**H_2Ph), 34.33 (**C**H_3); **LRMS (+ESI)** 491 [(M + Na)$^+$ 100%], 469 [(M + H)$^+$ 50%]; **IR (νmax/cm^{-1})** 3051, 2930, 1650, 1593, 1562, 1487, 1473, 1458, 1435, 1402, 1366, 1290, 1217, 1154, 1097, 1074, 1047, 997, 875, 811, 692, 596, 421; Found: C, 74.32; H, 5.38; N, 5.92 Calc for $C_{29}H_{25}ClN_2O_2$: C, 74.27; H, 5.37; N, 5.97%

2-(3-(3-Chlorophenyl)-9*H*-carbazol-9-yl)-*N*-(3-methoxybenzyl)-*N*-methylacetamide (20b). White solid; yield 69% (52 mg, 0.111 mmol). $\mathbf{R_f}$ 0.50 (ethyl acetate/hexane, 3:7 v/v); **^{1}H NMR (400 MHz,**

$CDCl_3$) δ = 8.25 (s, 1H, Ar**H**), 8.20 – 8.02 (m, 2H, Ar**H**), 7.74 – 7.54 (m, 3H, Ar**H**), 7.51 – 7.19 (m, 6H, Ar**H**), 6.95 – 6.63 (m, 3H, Ar**H**), 5.12 (s, 2H, C**H_2**CO), 4.61 (s, 2H, C**H_2**Ph), 3.73 (s, 3H, OC**H_3**), 2.97 (s, 3H, C**H_3**); **^{13}C NMR (101 MHz, $CDCl_3$) δ =** 167.24 (**C**O), 159.96 (Ar), 143.91 (Ar), 141.16 (Ar), 138.18 (Ar), 137.42 (Ar), 135.27 (Ar), 134.45 (Ar), 133.65 (Ar), 133.00 (Ar), 129.94 (Ar), 129.59 (Ar), 127.31 (Ar), 126.43 (Ar), 126.23 (Ar), 125.41 (Ar), 123.81 (Ar), 123.25 (Ar), 120.55 (Ar), 119.86 (Ar), 119.07 (Ar), 118.01 (Ar), 113.36 (Ar), 111.65 (Ar), 108.67 (Ar), 55.19 (O**C**H_3), 51.63 (**C**H_2CO), 45.62 (**C**H_2Ph), 34.31 (**C**H_3); **LRMS (+ESI)** 491 [$(M + Na)^+$ 100%], 469 [$(M + H)^+$ 50%]; **IR (νmax/cm^{-1})** 3051, 2931, 1652, 1592, 1562, 1458, 1435, 1403, 1365, 1327, 1256, 1215, 1153, 1097, 1074, 1046, 939, 873, 812, 691, 604, 420; Found: C, 74.29; H, 5.41; N, 5.96 Calc for $C_{29}H_{25}ClN_2O_2$: C, 74.27; H, 5.37; N, 5.97%

2-(3-(4-Chlorophenyl)-9*H*-carbazol-9-yl)-*N*-(3-methoxybenzyl)-*N*-methylacetamide (20c). White solid; yield 65% (49 mg, 0.105 mmol). **R_f** 0.32 (ethyl acetate/hexane, 3:7 v/v); **^{1}H NMR (400 MHz, $CDCl_3$) δ =** 8.28 (s, 1H, Ar**H**), 8.16 (d, *J* = 7.7 Hz, 1H, Ar**H**), 7.71 – 7.60 (m, 3H, Ar**H**), 7.52 – 7.35 (m, 4H, Ar**H**), 7.32 – 7.21 (m, 3H, Ar**H**), 6.97 – 6.63 (m, 3H, Ar**H**), 5.13 (s, 2H, C**H_2**CO), 4.62 (s, 2H, C**H_2**Ph), 3.73 (s, 3H, OC**H_3**), 2.97 (s, 3H, C**H_3**); **^{13}C NMR (101 MHz, $CDCl_3$) δ =** 167.16 (**C**O), 159.96 (Ar), 141.19 (Ar), 140.55 (Ar), 138.25 (Ar), 132.51 (Ar), 130.27 (Ar), 129.66 (Ar), 128.85 (2×Ar), 128.50 (2×Ar), 126.28 (Ar), 125.26 (Ar), 123.81 (Ar), 123.26 (Ar), 120.56 (Ar), 120.48 (Ar), 119.79 (Ar), 119.67 (Ar), 118.91 (Ar), 118.03 (Ar), 113.35 (Ar), 111.63 (Ar), 108.83 (Ar), 55.18 (O**C**H_3), 51.59 (**C**H_2CO), 45.66 (**C**H_2Ph), 34.29 (**C**H_3); **LRMS (+ESI)** 491 [$(M + Na)^+$ 100%], 469 [$(M + H)^+$ 50%]; **IR (νmax/cm^{-1})** 3049, 2929, 1647, 1593, 1561, 1487, 1474, 1459, 1436, 1402, 1367, 1290, 1217, 1155, 1093, 1073, 1046, 997, 875, 811, 692, 596, 420; Found: C, 74.33; H, 5.39; N, 5.93 Calc for $C_{29}H_{25}ClN_2O_2$: C, 74.27; H, 5.37; N, 5.97%

Membrane preparation. Stably transfected TSPO WT and TSPO A147T HEK293 cells were generated by Dr. Sook Wern Chua and Prof. Lars Ittner (University of New South Wales, NSW, Australia). The generation and validation of these cells as adequate models of in situ high affinity and low affinity binders are detailed in Sokias *et al.*[19] HEK 293 cells over-expressing TSPO WT and A147T were

incubated with phosphate buffered saline (Sigma Aldrich) containing 0.04% EDTA (pH 7.4) at 37 °C for 10 min to detach the cells. Cells were centrifuged at 1200 rpm for 5 min at 20 °C and resuspended in 5 mM of ice-cold Tris-HCl (Sigma Aldrich). The pellets were homogenized (Ultra-Turrax homogen**ize**r, IKA Weke, Staufen, Germany) on ice. The homogenates were centrifuged at 48000 *g* at 4 °C for 15 min. This step was repeated three times. After each spin, the supernatants were discarded and the pellets resuspended in 50 mM Tris-HCl. The final protein concentration of the pellets was determined using a bicinchoninic acid protein assay (Pierce Biotechnology Inc., Rockford IL) according to manufacturer's protocol. Absorbance was measured using a POLARstar Omega plate reader (BMG Labtech, Durham NC).

Competition radioligand binding assay. Competition radioligand binding was performed as previously described by Sokias *et al.*,[19] with some modifications as described below. Membranes expressing TSPO WT (20 µg/well) or TSPO A147T (10 µg/well) were incubated with 10 nM [^{3}H]PK 11195 (S.A. 85.1 Ci/mmol; Perkin Elmer) in the presence of novel ligands at logarithmically-spaced concentrations between 3.1 nM-10 µM for 90 min at 4 °C. Non-specific binding was determined in the presence of a saturating concentration of 1 µM PK 11195 (Sigma). The incubation was terminated by rapid filtration through a 96-well glass-fibre filter plate (G/FC grade; Millipore). The plates were washed with 50 mM Tris-HCl (pH 7.4) at 4 °C using a Brandel 96-sample vacuum harvester (Gaithersburg, MD, USA). The filters were covered with MicroScint 0 scintillation cocktail (Perkin Elmer). Radioactivity was measured using Microbeta^2 2450 Microplate counter (Perkin Elmer). Binding affinity (Ki) was determined using a one-site competitive binding fit in GraphPad Prism 7.02 software (GraphPad Software Inc., San Diego, CA, USA). Data were expressed as mean ± S.D from at least three independent experiments.

Whole cell radioligand binding assay. Binding was performed according to the competition radioligand binding assay detailed above, with the following amendments. Instead of using membranes extracted from TSPO WT and A147T, whole cells were used. Cells were detached using 0.04% PBS-

EDTA (pH 7.4) for 5 min at 37 °C. Cells were spun at 1200 rpm for 5 min at 20 °C and resuspended in 50 mM Tris-HCl. $1x10^6$ cells were treated with novel ligands and 10 nM [^{3}H]PK 11195. The binding affinity of three lead novel ligands were determined.

Cell viability. The metabolism of resazurin, a cell-permeable redox indicator, was used to determine the proportion of viable cells after exposure of compound. Viable cells are able to metabolize resazurin into resorufin, a fluorescent end product. TSPO WT and A147T HEK-293 cells (8.75 x 103 cells/ well) were incubated in poly-L-lysine-coated (100 µg/mL) plates for 24 h. Cells were treated with drugs for 48 h, after which resazurin-containing CellTiter Blue (20 µL, Promega, Madison, WI) was added to the cells and incubated at 37°C for 4 h, as per the manufacturer's instructions. Supernatants (100 µL) were transferred into a black-well plate and the fluorescence was measured using a POLARstar Omega plate reader at 530 nm (ex)/ 590 nm (em). All data were normalized to vehicle-treated controls. Values represent mean ± SEM of three independent experiments. Statistical analysis was performed using GraphPad Prism 7.02, with two-way ANOVA followed by Dunnett's multiple comparison test. $p< 0.05$ was considered statistically significant. (Figure 2A, ANOVA $F_{(9,36)} = 8.194$, $P< 0.001$)

BrdU ELISA. Cell proliferation was assayed by an ELISA which measures the incorporation of bromodeoxyuridine (BrdU) into newly synthesized DNA of replicating cells. TSPO WT or A147T HEK-293 cells (8.75 x 103 cells/ well) were incubated in poly-L-lysine-coated (100 µg/mL) plates for 24 h. Test compounds were added and incubated for a further 48 h. BrdU (Roche Molecular Diagnostics, Indianapolis, IN) was added to the culture sample at 37 °C for 4 h, and then a BrdU ELISA was performed according to the manufacturer's instructions (Roche Molecular Diagnostics). The reaction was stopped with 1 M sulfuric acid and the absorbance was measured with a POLARstar Omega plate reader (BMG, Labtech, Durham, NC) at 450 nm. All data were normalized to vehicle-treated controls. Statistical significance was assessed with GraphPad Prism 7.02 using a two-way ANOVA with Dunnett's multiple comparison test (Figure 2B, ANOVA $F_{(9,60)} = 28.82$, $p< 0.001$, Figure 2C, ANOVA $F_{(9,40)} = 8.528$, $P< 0.001$).

Pregnenolone ELISA. Steroidogenic activity was measured using a rat C6 glioma cell line. Cells were plated into a 96 well plate at 1 x 10^5 cells/ well. After 24 h, cells were washed twice with ELISA buffer (140 mM NaCl, 5 mM KCl, 1.8 mM $CaCl_2$, 1 mM $MgSO_4$, 10 mM glucose, 10 mM HEPES-NaOH, pH 7.4, and 0.1% bovine serum albumin). The amount of pregnenolone released into the buffer was measured by incubating TSPO ligands (100 μM) in ELISA buffer for 2 h. Pregnenolone synthesis inhibitors, trilostane (25 μM, Sigma) and SU10603 (10 μM, Muse Chem) were added to the ELISA buffer. DMSO (0.1%) was used as a vehicle control. The buffer was then extracted and centrifuged at 1500 *g* for 10 min at 20 °C. The amount of pregnenolone released was measured using a pregnenolone ELISA (IBL International) accorded to the manufacturer's protocol. Values represent mean ± SD of three independent experiments. Statistical significance was assessed with GraphPad Prism 7.02 using a one-way ANOVA with Dunnett's multiple comparison test (Figure 4, ANOVA $F(3,10) = 62.41$).

Homology modelling. The protein sequence for the human TSPO protein was obtained from sequencing. The crystal structure of the TSPO protein from Bacillus cereus (PDB ID: 4RYI) was used as the structural template to build the homology model. Homology modelling was performed using the Prime v5.4[29] software, within the Schrödinger software suite.

Target protein preparation. The homology model was prepared using preparation and refinement protocols, directed by the Protein Preparation Wizard[30] embedded in Maestro v11.8 (Schrödinger, LLC, New York, USA). This process includes assigning bond orders, adding hydrogen atoms, and creating zero-order bonds to metals and disulphide bonds. The hydrogen bond network within the protein was also optimized with all het groups within the receptor grid bounding box previously removed and the protein structure minimized to a root mean square deviation (RMSD) of 0.3 Å using the OPLS3force field.[31] The ligands studied were prepared using Ligprep v4.9[32] to generate possible stereoisomers of the ligands as well as generating all potential ionization states at pH 7±2. Confgen[33] v4,7 was utilized to obtain up to 64 different conformers for each ligand and each ligand.

Receptor grid generation. The Receptor Grid Generation tool in Glide v8.1[34] was used to characterize the binding site for the docking studies. Binding sites were defined by a 20 Å[31] bounding box centered at the ligand co-crystallized in the protein. A Coulomb-van der Waals scaling factor of 1.0 for receptor van der Waals radii was applied to protein atoms with a partial charge of less than 0.25 and a similar factor of 0.8 was applied to ligand atoms with a partial charge cutoff of less than 0.15 e. Rotations of hydroxyl and thiol groups were not allowed.

Docking studies. The ligands were docked into the receptor grids with Glide v8.1.[34] All docking was carried out using the Extra Precision (XP) scoring function to refine binding energy estimates. All ligands were docked with flexible states to allow sampling of the effect of nitrogen inversion, changing ring conformations and non-planar amide functional groups were penalized. PrimeMM-GBSA calculations which combines molecular mechanics (MM) terms, and a generalized Born and surface area (GBSA) solvent mode,[20] was utilized to calculate the free energy of binding for the ligands. A water molecules was used as the probe. The output poses from Glide XP docking were used as the basis for these calculations. The calculations were performed using the variable-dielectric generalized Born (VSGB) solvation model and OPLS3 force field. The protein was kept rigid for these calculations while the docked ligand was allowed to be flexible.

ASSOCIATED CONTENT

Supporting Information. The Supporting Information is available free of charge on the ACS Publications website.

- Experimental procedures for the preparation of the non-commercially available secondary amines and alkylating agents.
- Docking and MM-GBSA dG binding scores and key interacting residues for selected ligands (**8b, 15a, 19b, 20a).** Ligand binding diagrams for ligands, **19b** and **20a**.
- NMR spectra for selected ligands (**6b, 7a, 7c, 8b, 19a, 19c**)
- Molecular Formula Strings (CSV).

AUTHOR INFORMATION

Corresponding Author

* M.K. Telephone: +61 2 9351 2745. Fax: +61 2 9351 3329. Email: michael.kassiou@sydney.edu.au.

Author Contributions

H.W.A.C and R.S are co-first-authors[§], contributing equally to this work. E.W assisted with the pharmacological screening while T.A.R and M.K assisted with the design and synthesis of ligands. The transfected HEK293 cells were provided by L.M.I. Q.G, J.D and D.E.H provided the TSPO docking studies for ligands **8b**, **15a**, **19b** and **20a**. All authors contributed to the writing and proof-reading of the manuscript.

Funding Sources

This work was supported in part by the National Health and Medical Research Council of Australia.

ACKNOWLEDGEMENT

We wish to acknowledge Dr Donna Lai and Dr Sheng Hua for assistance with equipment in the Bosch Molecular Biology Facility.

ABBREVIATIONS USED

Ala, alanine; Cs_2CO_3, caesium carbonate; CH_2Cl_2, dichloromethane; DIPEA, diisopropylethylamine; DMF, dimethylformamide; EtOAc, ethyl acetate; HAB, high affinity binders; h, hours; HEK, human embryonic kidney; H_2, hydrogen gas; K_i, inhibitor constant; kDa, kilodalton; LiOH, lithium hydroxide; LAB, low affinity binders; MeOH, methanol; μM, micromolar; nm, nanomolar; HBTU, *N,N,N′,N′*-tetramethyl-*O*-(1H-benzotriazol-1-yl)uronium hexafluorophosphate; Pd/C, palladium on carbon; PET, positron emission tomography; KOtBu, potassium *tert*-butoxide; rt, room temperature; SNP, single nucleotide polymorphism; NaCl, sodium chloride; NaH, sodium hydride; SD, standard deviation; $Pd(PPh_3)_4$, tetrakis(triphenylphosphine)palladium(0); Thr, Threonine; TSPO, translocator protein; H_2O, water; WT, wild type.

REFERENCES

1. Papadopoulos, V.; Baraldi, M.; Guilarte, T. R.; Knudsen, T. B.; Lacapere, J. J.; Lindemann, P.; Norenberg, M. D.; Nutt, D.; Weizman, A.; Zhang, M. R.; Gavish, M., Translocator protein (18kDa): new nomenclature for the peripheral-type benzodiazepine receptor based on its structure and molecular function. *Trends Pharmacol Sci* **2006,** *27* (8), 402-409.

2. Biswas, L.; Farhan, F.; Reilly, J.; Bartholomew, C.; Shu, X., TSPO ligands promote cholesterol efflux and suppress oxidative stress and inflammation in choroidal endothelial cells. *Int J Mol Sci* **2018,** *19* (12).

3. Gavish, M.; Bachman, I.; Shoukrun, R.; Katz, Y.; Veenman, L.; Weisinger, G.; Weizman, A., Enigma of the peripheral benzodiazepine receptor. *Pharmacol Rev* **1999,** *51* (4), 629-650.

4. Owen, D. R.; Matthews, P. M., Imaging brain microglial activation using positron emission tomography and translocator protein-specific radioligands. *Int Rev Neurobiol* **2011,** *101*, 19-39.

5. Owen, D. R.; Yeo, A. J.; Gunn, R. N.; Song, K.; Wadsworth, G.; Lewis, A.; Rhodes, C.; Pulford, D. J.; Bennacef, I.; Parker, C. A.; StJean, P. L.; Cardon, L. R.; Mooser, V. E.; Matthews, P. M.; Rabiner, E. A.; Rubio, J. P., An 18-kDa translocator protein (TSPO) polymorphism explains differences in binding affinity of the PET radioligand PBR28. *J Cereb Blood Flow Metab* **2012,** *32* (1), 1-5.

6. Owen, D. R.; Gunn, R. N.; Rabiner, E. A.; Bennacef, I.; Fujita, M.; Kreisl, W. C.; Innis, R. B.; Pike, V. W.; Reynolds, R.; Matthews, P. M.; Parker, C. A., Mixed-affinity binding in humans with 18-kDa translocator protein ligands. *J Nucl Med* **2011,** *52* (1), 24-32.

7. Owen, D. R.; Lewis, A. J.; Reynolds, R.; Rupprecht, R.; Eser, D.; Wilkins, M. R.; Bennacef, I.; Nutt, D. J.; Parker, C. A., Variation in binding affinity of the novel anxiolytic XBD173 for the 18 kDa translocator protein in human brain. *Synapse* **2011,** *65* (3), 257-259.

8. Guo, Q.; Colasanti, A.; Owen, D. R.; Onega, M.; Kamalakaran, A.; Bennacef, I.; Matthews, P. M.; Rabiner, E. A.; Turkheimer, F. E.; Gunn, R. N., Quantification of the specific translocator protein signal of 18F-PBR111 in healthy humans: a genetic polymorphism effect on in vivo binding. *J Nucl Med* **2013,** *54* (11), 1915-1923.

9. Rojas, C.; Stathis, M.; Coughlin, J. M.; Pomper, M.; Slusher, B. S., The low-affinity binding of second generation radiotracers targeting TSPO is associated with a unique allosteric binding site. *J Neuroimmune Pharmacol* **2018,** *13* (1), 1-5.

10. Zanotti-Fregonara, P.; Zhang, Y.; Jenko, K. J.; Gladding, R. L.; Zoghbi, S. S.; Fujita, M.; Sbardella, G.; Castellano, S.; Taliani, S.; Martini, C.; Innis, R. B.; Da Settimo, F.; Pike, V. W., Synthesis and evaluation of translocator 18 kDa protein (TSPO) positron emission tomography (PET) radioligands with low binding sensitivity to human single nucleotide polymorphism rs6971. *ACS Chem Neurosci* **2014,** *5* (10), 963-971.

11. Vivash, L.; O'Brien, T. J., Imaging microglial activation with TSPO PET: Lighting up neurologic diseases? *J Nucl Med* **2016,** *57* (2), 165-168.

12. Fan, Z.; Calsolaro, V.; Atkinson, R. A.; Femminella, G. D.; Waldman, A.; Buckley, C.; Trigg, W.; Brooks, D. J.; Hinz, R.; Edison, P., Flutriciclamide (18F-GE180) PET: first-in-human PET study of novel third-generation in vivo marker of human translocator protein. *J Nucl Med* **2016,** *57* (11), 1753-1759.

13. Cheung, Y. Y.; Nickels, M. L.; Tang, D.; Buck, J. R.; Manning, H. C., Facile synthesis of SSR180575 and discovery of 7-chloro-N,N,5-trimethyl-4-oxo-3(6-[(18)F]fluoropyridin-2-yl)-3,5-dihydro-4H-pyri dazino[4,5-b]indole-1-acetamide, a potent pyridazinoindole ligand for PET imaging of TSPO in cancer. *Bioorg Med Chem Lett* **2014,** *24* (18), 4466-4471.

14. Gluszynska, A., Biological potential of carbazole derivatives. *Eur J Med Chem* **2015,** *94*, 405-26.

15. Wang, J.; Zheng, Y.; Efferth, T.; Wang, R.; Shen, Y.; Hao, X., Indole and carbazole alkaloids from Glycosmis montana with weak anti-HIV and cytotoxic activities. *Phytochemistry* **2005,** *66* (6), 697-701.

16. Knolker, H. J.; Reddy, K. R., Isolation and synthesis of biologically active carbazole alkaloids. *Chem Rev* **2002,** *102* (11), 4303-4427.

17. Farges, R.; Joseph-Liauzun, E.; Shire, D.; Caput, D.; Le Fur, G.; Ferrara, P., Site-directed mutagenesis of the peripheral benzodiazepine receptor: identification of amino acids implicated in the binding site of Ro5-4864. *Mol Pharmacol* **1994,** *46* (6), 1160-1157.

18. Jaremko, L.; Jaremko, M.; Giller, K.; Becker, S.; Zweckstetter, M., Structure of the mitochondrial translocator protein in complex with a diagnostic ligand. *Science* **2014,** *343* (6177), 1363-1366.

19. Sokias, R.; Werry, E. L.; Chua, S. W.; Reekie, T. A.; Munoz, L.; Wong, E. C. N.; Ittner, L. M.; Kassiou, M., Determination and reduction of translocator protein (TSPO) ligand rs6971 discrimination. *Medchemcomm* **2017,** *8* (1), 202-210.

20. Lyne, P. D.; Lamb, M. L.; Saeh, J. C., Accurate prediction of the relative potencies of members of a series of kinase inhibitors using molecular docking and MM-GBSA scoring. *J Med Chem* **2006,** *49* (16), 4805-4808.

21. Ryu, J. K.; Choi, H. B.; McLarnon, J. G., Peripheral benzodiazepine receptor ligand PK11195 reduces microglial activation and neuronal death in quinolinic acid-injected rat striatum. *Neurobiol Dis* **2005,** *20* (2), 550-561.

22. Werry, E. L.; Barron, M. L.; Kassiou, M., TSPO as a target for glioblastoma therapeutics. *Biochem Soc Trans* **2015,** *43* (4), 531-536.

23. Narlawar, R.; Werry, E. L.; Scarf, A. M.; Hanani, R.; Chua, S. W.; King, V. A.; Barron, M. L.; Martins, R. N.; Ittner, L. M.; Rendina, L. M.; Kassiou, M., First demonstration of positive allosteric-like modulation at the human wild type translocator protein (TSPO). *J Med Chem* **2015,** *58* (21), 8743-8749.

24. Costa, B.; Da Pozzo, E.; Giacomelli, C.; Taliani, S.; Bendinelli, S.; Barresi, E.; Da Settimo, F.; Martini, C., TSPO ligand residence time influences human glioblastoma multiforme cell death/life balance. *Apoptosis* **2015,** *20* (3), 383-398.

25. Da Pozzo, E.; Costa, B.; Martini, C., Translocator protein (TSPO) and neurosteroids: implications in psychiatric disorders. *Curr Mol Med* **2012,** *12* (4), 426-442.

26. Wolf, L.; Bauer, A.; Melchner, D.; Hallof-Buestrich, H.; Stoertebecker, P.; Haen, E.; Kreutz, M.; Sarubin, N.; Milenkovic, V. M.; Wetzel, C. H.; Rupprecht, R.; Nothdurfter, C., Enhancing neurosteroid synthesis--relationship to the pharmacology of translocator protein (18 kDa) (TSPO) ligands and benzodiazepines. *Pharmacopsychiatry* **2015,** *48* (2), 72-77.

27. Verleye, M.; Akwa, Y.; Liere, P.; Ladurelle, N.; Pianos, A.; Eychenne, B.; Schumacher, M.; Gillardin, J. M., The anxiolytic etifoxine activates the peripheral benzodiazepine receptor and increases the neurosteroid levels in rat brain. *Pharmacol Biochem Behav* **2005,** *82* (4), 712-720.

28. Bitran, D.; Foley, M.; Audette, D.; Leslie, N.; Frye, C. A., Activation of peripheral mitochondrial benzodiazepine receptors in the hippocampus stimulates allopregnanolone synthesis and produces anxiolytic-like effects in the rat. *Psychopharmacology (Berl)* **2000,** *151* (1), 64-71.

29. Jacobson, M. P.; Pincus, D. L.; Rapp, C. S.; Day, T. J.; Honig, B.; Shaw, D. E.; Friesner, R. A., A hierarchical approach to all-atom protein loop prediction. *Proteins* **2004,** *55* (2), 351-367.

30. Sastry, G. M.; Adzhigirey, M.; Day, T.; Annabhimoju, R.; Sherman, W., Protein and ligand preparation: parameters, protocols, and influence on virtual screening enrichments. *J Comput Aided Mol Des* **2013,** *27* (3), 221-234.

31. Harder, E.; Damm, W.; Maple, J.; Wu, C.; Reboul, M.; Xiang, J. Y.; Wang, L.; Lupyan, D.; Dahlgren, M. K.; Knight, J. L.; Kaus, J. W.; Cerutti, D. S.; Krilov, G.; Jorgensen, W. L.; Abel, R.; Friesner, R. A., OPLS3: A force field providing broad coverage of drug-like small molecules and proteins. *J Chem Theory Comput* **2016,** *12* (1), 281-296.

32. Schrödinger. Ligprep, version 4.9. New York, NY: Schrödinger, LLC; 2018.

33. Watts, K. S.; Dalal, P.; Murphy, R. B.; Sherman, W.; Friesner, R. A.; Shelley, J. C., ConfGen: a conformational search method for efficient generation of bioactive conformers. *J Chem Inf Model* **2010,** *50* (4), 534-546.

34. Friesner, R. A.; Murphy, R. B.; Repasky, M. P.; Frye, L. L.; Greenwood, J. R.; Halgren, T. A.; Sanschagrin, P. C.; Mainz, D. T., Extra precision glide: docking and scoring incorporating a model of hydrophobic enclosure for protein-ligand complexes. *J Med Chem* **2006,** *49* (21), 6177-6196.

Table of Contents Graphic

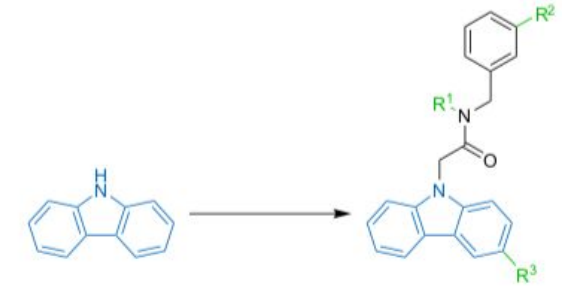

Readily accessible starting material

Non-discriminating and improved TSPO binding

Ligand	TSPO K_i (nM)		A147T:WT
	A147T	WT	
PK 11195	26.7 ± 4.5	22.5 ± 5.2	1.2
R^1 = Et R^2 = OMe R^3 = H	100.4 ± 22.5	96.1 ± 30.4	1.0
R^1 = Me R^2 = OMe R^3 = 4-OMePh	25.4 ± 8.2	6.6 ± 2.2	3.8

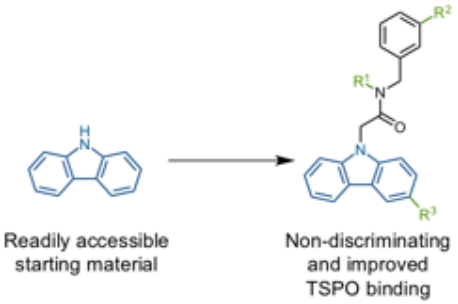

Ligand	TSPO K_i (nM)		A147T: WT
	A147T	WT	
PK 11195	26.7 ± 4.5	22.5 ± 5.2	1.2
$R^1 = CH_2CH_3$ R^2 = OMe R^3 = H	100.4 ± 22.5	96.1 ± 30.4	1.0
$R^1 = CH_3$ R^2 = OMe R^3 = 4-OMePh	25.4 ± 8.2	6.6 ± 2.2	3.8